

# Editing the core region in HPFH deletions alters fetal and adult globin expression for treatment of $\beta$ -hemoglobinopathies

Vigneshwaran Venkatesan,<sup>1,2</sup> Abisha Crystal Christopher,<sup>1</sup> Manuel Rhiel,<sup>3,4</sup> Manoj Kumar K. Azhagiri,<sup>1,2</sup> Prathibha Babu,<sup>1,2</sup> Kaivalya Walavalkar,<sup>5</sup> Bharath Saravanan,<sup>5</sup> Geoffroy Andrieux,<sup>6,7</sup> Sumathi Rangaraj,<sup>1</sup> Saranya Srinivasan,<sup>1</sup> Karthik V. Karuppusamy,<sup>1,2</sup> Annlin Jacob,<sup>1</sup> Abhirup Bagchi,<sup>1</sup> Aswin Anand Pai,<sup>8</sup> Yukio Nakamura,<sup>9</sup> Ryo Kurita,<sup>9</sup> Poonkuzhali Balasubramanian,<sup>8</sup> Rekha Pai,<sup>10</sup> Srujan Kumar Marepally,<sup>1</sup> Kumarasamypet Murugesan Mohankumar,<sup>1</sup> Shaji R. Velayudhan,<sup>1,8</sup> Melanie Boerries,<sup>6,7</sup> Dimple Notani,<sup>5</sup> Toni Cathomen,<sup>3,4</sup> Alok Srivastava,<sup>1,8</sup> and Saravanabhavan Thangavel<sup>1</sup>

<sup>1</sup>Centre for Stem Cell Research (CSCR), A Unit of InStem Bengaluru, Christian Medical College Campus, Vellore, Tamil Nadu 632002, India; <sup>2</sup>Manipal Academy of Higher Education, Manipal 576104, Karnataka, India; <sup>3</sup>Institute for Transfusion Medicine and Gene Therapy, Medical Center – University of Freiburg, 79106 Freiburg, Germany; <sup>4</sup>Center for Chronic Immunodeficiency, Medical Faculty, University of Freiburg, 79106 Freiburg, Germany; <sup>5</sup>National Centre for Biological Sciences, Tata Institute of Fundamental Research, Bangalore, Karnataka 560065, India; <sup>6</sup>Institute of Medical Bioinformatics and Systems Medicine, Faculty of Medicine & Medical Center - University of Freiburg, 79106 Freiburg, Germany; <sup>7</sup>German Cancer Consortium (DKTK), Partner Site Freiburg and German Cancer Research Center (DKFZ), 69120 Heidelberg, Germany; <sup>8</sup>Department of Hematology, Christian Medical College, Vellore, Tamil Nadu 632004, India; <sup>9</sup>Cell Engineering Division, RIKEN BioResource Research Center, Ibaraki 3050074, Japan; <sup>10</sup>Department of Pathology, Christian Medical College, Vellore, Tamil Nadu 632004, India

**Reactivation of fetal hemoglobin (HbF) is a commonly adapted strategy to ameliorate  $\beta$ -hemoglobinopathies. However, the continued production of defective adult hemoglobin (HbA) limits HbF tetramer production affecting the therapeutic benefits. Here, we evaluated deletional hereditary persistence of fetal hemoglobin (HPFH) mutations and identified an 11-kb sequence, encompassing putative repressor region (PRR) to  $\beta$ -globin exon-1 ( $\beta$ E1), as the core deletion that ablates HbA and exhibits superior HbF production compared with HPFH or other well-established targets. PRR- $\beta$ E1-edited hematopoietic stem and progenitor cells (HSPCs) retained their genome integrity and their engraftment potential to repopulate for long-term hematopoiesis in immunocompromised mice producing HbF positive cells *in vivo*. Furthermore, PRR- $\beta$ E1 gene editing is feasible without *ex vivo* HSPC culture. Importantly, the editing induced therapeutically significant levels of HbF to reverse the phenotypes of both sickle cell disease and  $\beta$ -thalassemia major. These findings imply that PRR- $\beta$ E1 gene editing of patient HSPCs could lead to improved therapeutic outcomes for  $\beta$ -hemoglobinopathy gene therapy.**

## INTRODUCTION

$\beta$ -Hemoglobinopathies— $\beta$ -thalassemia and sickle cell disease (SCD)—are highly prevalent inherited globin chain disorders that are autosomal recessive. They account for 3.4% of mortalities in children younger than 5 years.<sup>1,2</sup>  $\beta$ -thalassemia is caused by more than 300 different mutations in the  $\beta$ -globin gene or its flanking nucleotides; these mutations impair the synthesis of the  $\beta$ -globin chain, affecting the tightly coordinated equilibrium of adult hemoglobin

(HbA/ $\alpha_2\beta_2$ ) chains.<sup>3</sup> The excess free  $\alpha$ -globin precipitates in erythroblasts and induces apoptosis, resulting in ineffective erythropoiesis.<sup>4</sup> SCD is caused by the E6V (rs334) missense mutation in the  $\beta$ -globin gene. This mutation causes polymerization of deoxygenated sickle hemoglobin (HbS) tetramers, which severely reduces the circulating lifespan of red blood cells (RBCs) and eventually causes vascular damage and progressive multiorgan damage.<sup>5</sup>

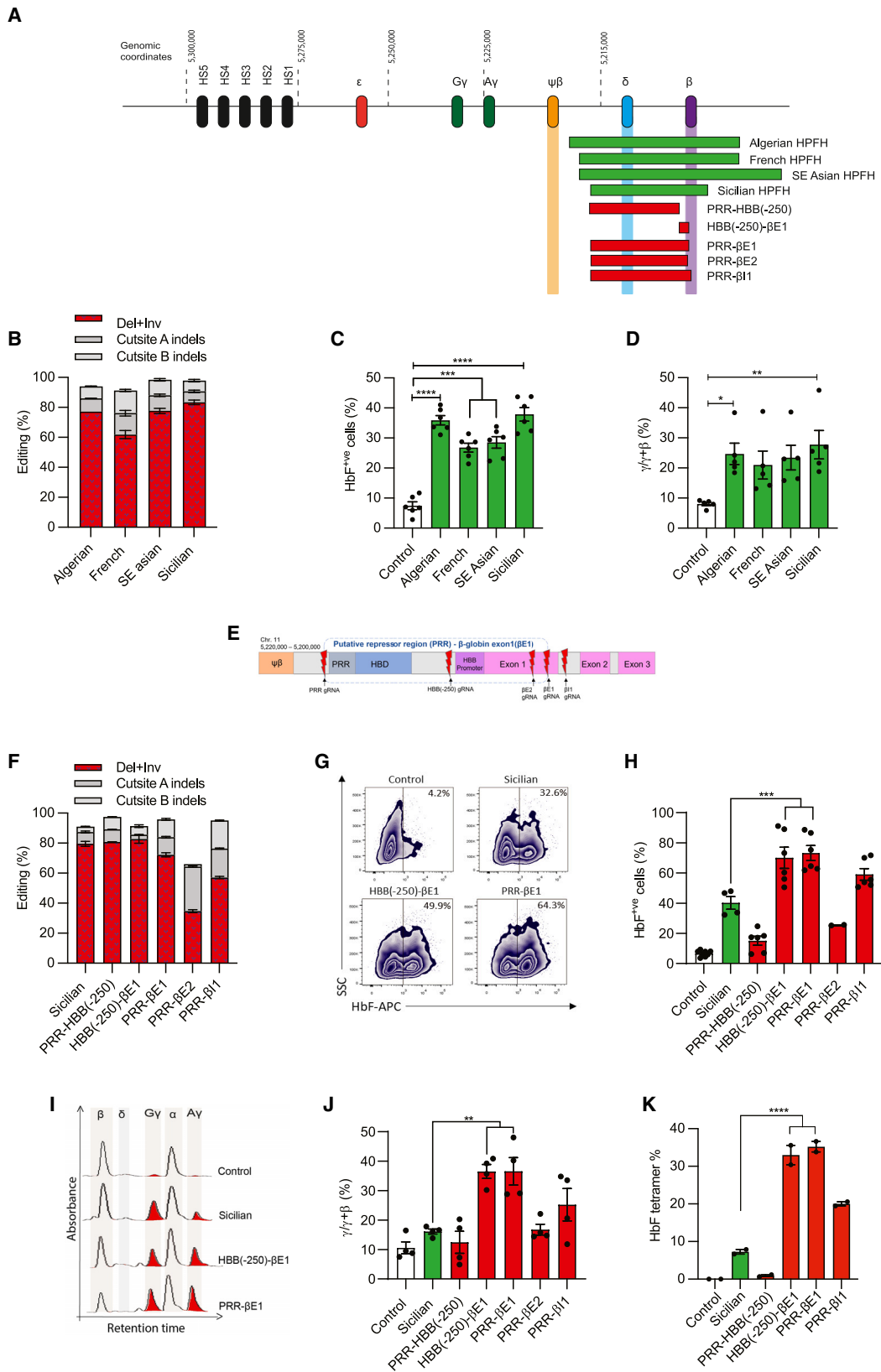
Morbidity in  $\beta$ -thalassemia and SCD patients is inversely correlated with the levels of fetal hemoglobin (HbF) in adulthood.<sup>6,7</sup> Expression of  $\gamma$ -globin, the fetal  $\beta$ -like globin component of HbF, improves the globin chain equilibrium and thus prevents apoptosis of erythroid cells in  $\beta$ -thalassemia. Similarly, in SCD,  $\gamma$ -globin competes with the sickle  $\beta$ -globin chains ( $\beta$ s) to form HbF tetramers ( $\alpha_2\gamma_2$ ), thereby reducing the production of sickle RBCs. Hence, several studies are focused on identifying and manipulating genetic factors involved in HbF regulation.<sup>8–10</sup> Two recent clinical studies involving short hairpin RNA (shRNA)-mediated erythroid-specific downregulation of BCL11A and gene-editing-mediated disruption of its erythroid-specific enhancer have demonstrated reactivated HbF levels sufficient to reach transfusion independence.<sup>11,12</sup> However, up to 50% of hemoglobin remained as HbS in the SCD patients; thus, strategies that reduce or eliminate defective  $\beta$ -globin production are worth further exploration.

Received 17 December 2022; accepted 24 April 2023;  
<https://doi.org/10.1016/j.omtn.2023.04.024>

**Correspondence:** Saravanabhavan Thangavel, Centre for Stem Cell Research (CSCR), A Unit of InStem Bengaluru, Christian Medical College Campus, Vellore, Tamil Nadu 632002, India.

**E-mail:** [sthangavel@cmcvellore.ac.in](mailto:sthangavel@cmcvellore.ac.in)





(legend on next page)

Mutations causing hereditary persistence of fetal hemoglobin (HPFH) are documented to produce varying levels of HbF in healthy individuals without any deleterious effects.<sup>13</sup> Importantly, the HPFH mutations are beneficial in alleviating disease severity when co-inherited with  $\beta$ -hemoglobinopathies.<sup>14</sup> Among the genetic variants that induce HbF expression, deletional HPFH mutations produce higher levels of HbF and are highly prevalent.<sup>15</sup>  $\beta$ -Globin production is ablated in HPFH deletions, distinguishing them from other HbF reactivating mutations. HPFH deletions range in size from 12.9 to 84.9 kb, encompassing *HBG1*, *HBBP1*, *HBD*, and *HBB* genes in the  $\beta$ -globin cluster, and result in pancellular HbF production.<sup>16</sup> The introduction of HPFH deletions in adult hematopoietic stem and progenitor cells (HSPCs) results in activation of  $\gamma$ -globin with subsequent amelioration of the sickle phenotype.<sup>17,18</sup> However, much is still unknown, such as the minimal genomic deletion required for therapeutically relevant  $\gamma$ -globin activation, genome integrity, engraftment, and repopulation potential of HSPCs harboring such genomic deletions and their efficacy in reversing the disease phenotype. In a very recent study, Topfer et al. showed that the deletion of the proximal promoter of *HBB*, excised in HPFH and  $\delta\beta$ -thalassemia deletions, is sufficient for  $\gamma$ -globin activation.<sup>19</sup>

To investigate the translational potential of HSPCs with deletional HPFH mutations, we used CRISPR-Cas9 to screen multiple HPFH deletions and identified an 11-kb core-regulatory region from putative repressor region (PRR) to  $\beta$ -globin exon-1 ( $\beta$ E1) (PRR- $\beta$ E1). Gene editing of PRR- $\beta$ E1 repressed the  $\beta$ -globin and activated  $\gamma$ -globin to levels greater than known candidates targeting the *BCL11A* enhancer and *HBB* promoter region, reversing the SCD and  $\beta$ -thalassemia phenotypes. We also demonstrated long-term hematopoiesis of the edited HSPCs and achieved efficient editing without cytokine pre-stimulation and genotoxicity.

## RESULTS

### Genomic deletion encompassing PRR to $\beta$ E1 is sufficient to reproduce deletional HPFH phenotype

To identify an HPFH deletion suitable for therapeutic gene editing, we introduced deletional HPFH mutations of <30 kb in size, mirroring the Algerian<sup>20</sup> (24 kb), French<sup>20</sup> (20 kb), Southeast (SE) Asian<sup>21</sup>

(27 kb), and Sicilian<sup>22</sup> (12.9 kb) genotypes, by CRISPR-Cas9 dual guide RNA (gRNA) gene editing in the HUDEP-2 cell line (Figure 1A). The 7.2-kb Corfu deletion, which is now considered as  $\delta\beta$ -thalassemia and requires homozygous deletion to activate therapeutic HbF levels,<sup>17,23</sup> was excluded from our screening. The efficiency of gene editing was assessed using droplet digital polymerase chain reaction (ddPCR) and Sanger sequencing in conjunction with Inference of CRISPR Edits (ICE) analysis.

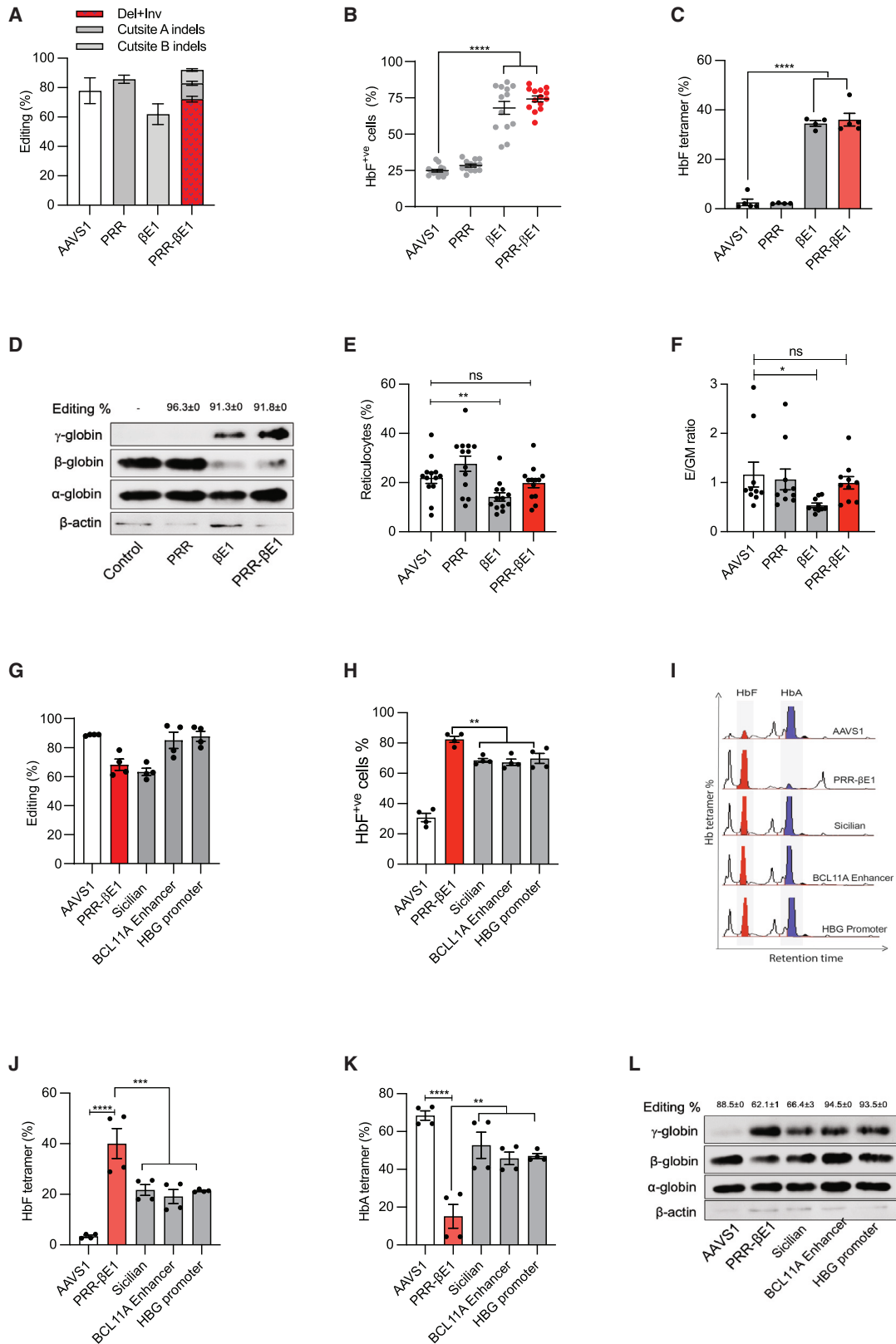
All candidates exhibited >60% editing efficiency (Figure 1B). Erythroid differentiation of gene-edited HUDEP-2 cells showed an increased percentage of HbF<sup>+</sup>ve cells (Figure 1C),  $\gamma$ -globin messenger RNA (mRNA) (Figure S1A), activation of  $\gamma$ -globin chains (Figure 1D), and decreased production of  $\beta$ -globin chains (Figure S1B) in all HPFH deletions. Sicilian HPFH produced a marginally higher level of  $\gamma$ -globin chains than the other targets, and is the central region among the HPFH deletions.

To decipher the HbF regulatory region in the Sicilian HPFH deletion, we excised different regions spanning the deletion, such as PRR to the upstream region of  $\beta$ -globin promoter (PRR-*HBB*(-250)), promoter to exon-1 (*HBB*(-250)- $\beta$ E1), PRR to exon-1 (PRR- $\beta$ E1), PRR to intron-1 (PRR- $\beta$ I1), and PRR to exon-1 CD27 (PRR- $\beta$ E2) of the  $\beta$ -globin gene (Figures 1A, 1E, and 1F). Among these candidates, *HBB*(-250)- $\beta$ E1 and PRR- $\beta$ E1 showed a 1.8-fold higher percentage of HbF<sup>+</sup>ve cells than the Sicilian HPFH (Figures 1G and 1H). Both candidates showed a substantial increase in the  $\gamma$ -globin activation (Figures 1I, 1J, and S1C) with decreased  $\beta$ -globin levels (Figure S1D). Sicilian HPFH favored G $\gamma$  activation, whereas the PRR- $\beta$ E1 and *HBB*(-250)- $\beta$ E1-edited cells displayed equivalent activation of both A $\gamma$  and G $\gamma$  chains (Figure S1E). Variant high-performance liquid chromatography (HPLC) analysis confirmed the functional HbF tetramer in both these samples, and they had a greater than 4-fold higher proportion of HbF tetramers than the Sicilian HPFH (Figure 1K).

To understand why Sicilian HPFH reactivates less  $\gamma$ -globin levels than *HBB*(-250)- $\beta$ E1 and PRR- $\beta$ E1, which are the regions within Sicilian HPFH, we single-cell sorted Sicilian HPFH edited HUDEP-2

### Figure 1. Genomic deletion encompassing PRR to $\beta$ E1 is sufficient to reproduce deletional HPFH phenotype

(A) Diagrammatic representation of  $\beta$ -globin cluster and the break points of naturally occurring HPFH deletions (green). These deletions are introduced in the experiments shown in (B)–(D). Break points of deletions (red) introduced in the experiment shown in (F)–(K). All these deletions were generated in HUDEP-2 cell lines by CRISPR-Cas9 dual gRNA approach. (B) Percentage of gene editing in HUDEP-2 cell lines, gene edited for HPFH deletions. Type of HPFH deletions are indicated at the x axis. Indels (cut site A and cut site B) measured by Sanger sequencing and ICE analysis. Deletion + Inversion (Del+Inv) (red checker box) quantified by ddPCR. n = 2. (C) Percentage of HbF<sup>+</sup>ve cells upon introducing HPFH deletions indicated on the x axis. The edited cells were differentiated into erythroblasts and analyzed for HbF by flow cytometry. n = 6. (D)  $\gamma$ -Globin chain synthesis as measured by  $\gamma/\gamma+\beta$  ratio in the HUDEP-2 erythroblasts as measured by HPLC chain analysis. n = 5. (E) Magnified image of  $\beta$ -globin locus showing the binding sites of the key gRNA employed in this study to create various deletions mentioned in (F)–(K). (F) Percentage of gene editing in HUDEP-2 cell lines gene edited for various deletions as indicated in the x axis. Indels (cut site A and cut site B) measured by Sanger sequencing and ICE analysis. Deletion + Inversion (Del+Inv) (red checker box) quantified by ddPCR. n = 2. (G) Representative flow cytometry plot of HbF<sup>+</sup>ve cells. HUDEP-2 cell lines gene edited for Sicilian HPFH deletion and deletion of its encompassing region in the  $\beta$ -globin cluster, were differentiated into erythroblasts and analyzed for HbF<sup>+</sup>ve cells. Inset shows percentage of HbF<sup>+</sup>ve cells. (H) Percentage of HbF<sup>+</sup>ve cells upon introducing deletions in the region encompassing Sicilian HPFH. n = 4. (I) Representative globin chain HPLC chromatograms. (J)  $\gamma$ -Globin chain synthesis as measured by  $\gamma/\gamma+\beta$  ratio in the HUDEP-2 cell lines as measured by HPLC chain analysis. n = 4. (K) Percentage of HbF tetramer in erythroid differentiated HUDEP-2 cells gene edited for introducing deletions in the region encompassing Sicilian HPFH as measured by variant HPLC analysis. n = 2. Error bars represent mean  $\pm$  SEM, \*p  $\leq$  0.05, \*\*p  $\leq$  0.01, \*\*\*p  $\leq$  0.001, \*\*\*\*p  $\leq$  0.0001 (one-way ANOVA followed by Dunnett's multiple comparisons test).



(legend on next page)

cells and generated clonal lines with inversion or deletions. Interestingly, HPLC analysis revealed intact  $\beta$ -globin expression and indicated no substantial increase of  $\gamma$ -globin in inversion clones. Contrastingly, clones with deletions exhibited decreased  $\beta$ -globin chains and activation of  $\gamma$ -globin. Similar trend was also observed with French HPFH (Figures S1F and S1G). This shows that inversion results in alterations of  $\beta$ -globin cluster orientation without impacting the  $\gamma$ -globin gene expression. Also, this observation explains why the  $\beta$ -globin levels are intact in Sicilian HPFH despite high gene editing efficiency. On the contrary, the inversion events on HBB(-250)- $\beta$ E1 and PRR- $\beta$ E1 editing disrupts the  $\beta$ -globin exonic regions and such events are reported to block the  $\beta$ -globin expression.<sup>18</sup>

The PRR- $\beta$ E1 region is excised in all the deletional HPFH mutations (Figure S2). The sequence spanning PRR is completely or partially intact in  $\delta\beta$ -thalassemia and  $\beta$ -thalassemia deletions, suggesting it as a region that distinguishes HPFH and thalassemia phenotypes. Whereas, HBB(-250)- $\beta$ E1 deletion resembles the British black and Croatian  $\beta$ -thalassemia genotypes<sup>24,25</sup> and was also reported recently as a target for HbF reactivation.<sup>19</sup> Therefore PRR- $\beta$ E1 was considered for further studies. The ddPCR-mediated quantification of PRR- $\beta$ E1 gene-editing analysis (Figures S3A and S3B) was further confirmed by gap PCR analysis in the sorted single-cell clones (Figures S3C and S3D).

### Robust $\gamma$ -globin induction and $\beta$ -globin silencing in the erythroblasts differentiated from PRR- $\beta$ E1-edited HSPCs

To investigate the effect of PRR- $\beta$ E1 editing in therapeutically relevant cells, granulocyte colony-stimulating factor (G-CSF)-mobilized HSPCs from five healthy donors were electroporated with Cas9 ribonucleoproteins (RNPs) targeting cut site A - PRR and cut site B -  $\beta$ E1 sites individually and in combination. The total gene-editing efficiency in PRR- $\beta$ E1 was  $92\% \pm 4\%$ , among which PRR- $\beta$ E1 deletion and inversion (del+inv) comprised  $72.1\% \pm 2\%$  (Figure 2A). The viability of PRR- $\beta$ E1-edited HSPCs remained similar to that of

AAVS1-edited cells (Figure S4A). Upon differentiation of HSPCs into erythroblasts using a three-phase *in vitro* erythroid differentiation protocol, a significant increase in the percentage of HbF<sup>+</sup>ve cells was observed in PRR- $\beta$ E1 ( $74.2\% \pm 3\%$ ) and  $\beta$ E1-edited cells ( $68.0\% \pm 3\%$ ) relative to the AAVS1 control ( $24.7\% \pm 3\%$ ) (Figure 2B). Variant HPLC analysis showed up to 13-fold higher levels of HbF tetramers and up to 5-fold reduced levels of HbA tetramers upon  $\beta$ E1 and PRR- $\beta$ E1 editing (Figures 2C and S4B). Consistent with all aforementioned analyses, RT-PCR analysis (Figure S4C) and western blot confirmed the increased  $\gamma$ -globin and decreased  $\beta$ -globin expression (Figures 2D and S4D), quantitatively confirming the absolute levels of  $\gamma$ -globin produced on PRR- $\beta$ E1 gene editing.

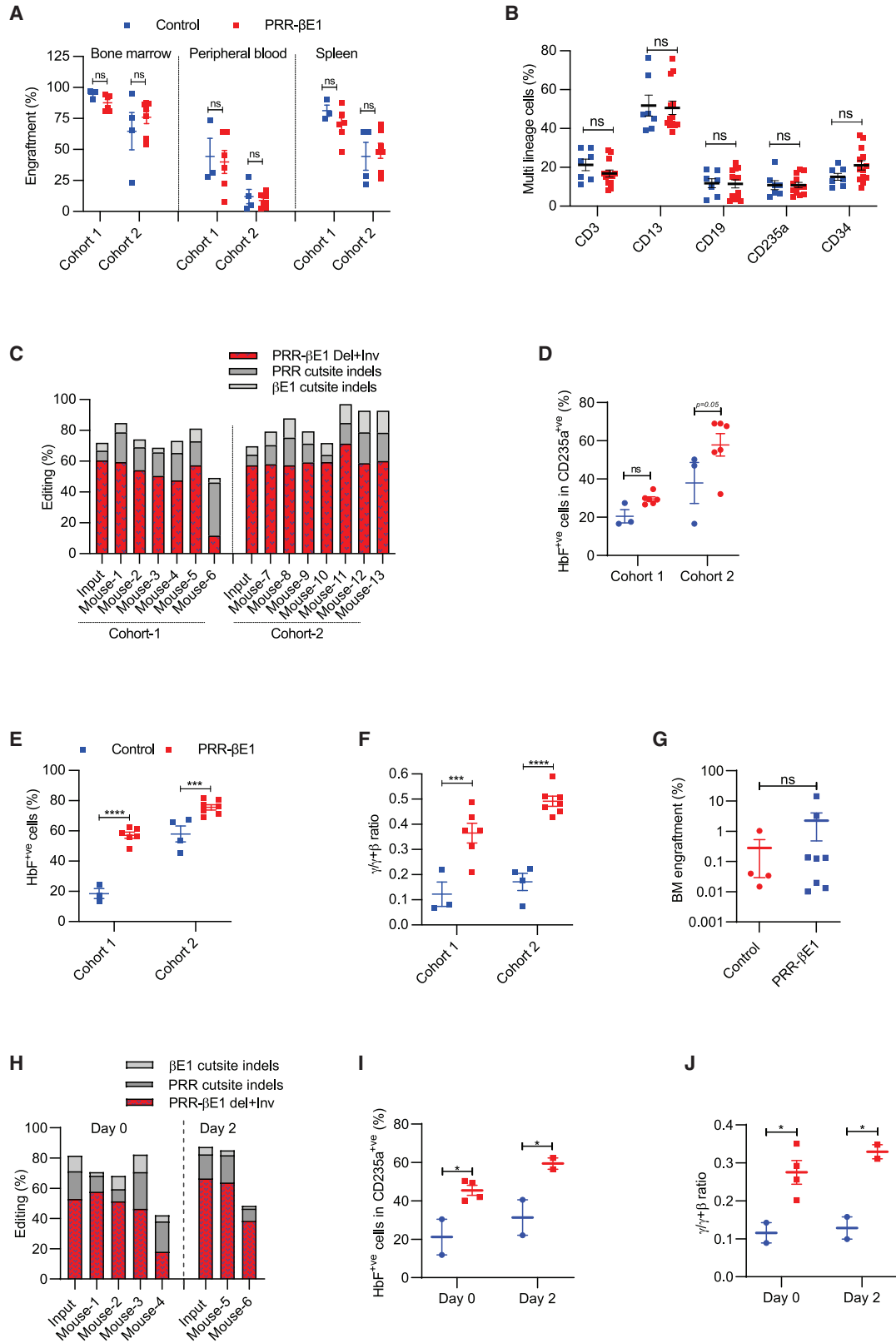
The frequency of gene editing in HSPCs and erythroblasts derived from gene-edited HSPCs did not differ significantly (Figure S4E). The erythroid maturation analysis using CD235a and Hoechst, showed that PRR- $\beta$ E1-edited cells had comparable levels of reticulocytes with the control, whereas the percentage of reticulocytes was significantly lower in  $\beta$ E1-edited cells (Figure 2E). A similar trend was observed with a different set of erythroid markers CD235a<sup>+</sup>/CD71<sup>-</sup> (Figure S4F).

Similarly, in PRR- $\beta$ E1 editing, erythroid colony-forming potential as assessed by the ratio of erythroid (Burst-forming unit [BFU-E] + colony-forming unit [CFU-E]) to granulocyte-monocyte (GM) generation, remained equivalent to AAVS1 but significantly decreased in  $\beta$ E1 editing (Figure 2F). All these analyses indicate normal erythropoiesis in PRR- $\beta$ E1 editing but not in  $\beta$ E1 editing.

We next compared the HbF induction by PRR- $\beta$ E1 and Sicilian HPFH with well-characterized targets: the BCL11A erythroid-specific enhancer and BCL11A-binding site in the *HBB* promoter that have advanced into clinical studies.<sup>12,26</sup> Gene-editing efficiencies and the ratio of erythroid to GM colonies were comparable for all these targets (Figures 2G and S4G). All four targets produced HbF<sup>+</sup>ve cells, with

### Figure 2. Robust $\gamma$ -globin induction and $\beta$ -globin silencing in the erythroblasts differentiated from PRR- $\beta$ E1-edited HSPCs

(A) Percentage of gene editing in PRR,  $\beta$ E1, and PRR- $\beta$ E1 gene-edited healthy donor HSPCs. Indels measured by Sanger sequencing and ICE analysis. Deletion + Inversion (Del+Inv) (red checker box) in PRR- $\beta$ E1 quantified by ddPCR. The PRR- $\beta$ E1-edited cells had deletion, indels at PRR region and  $\beta$ E1. Donor = 5, n = 11. (B) FACS analysis of percentage of HbF<sup>+</sup>ve cells in erythroblasts generated from gene-edited HSPCs. Gene-editing targets are indicated at the bottom. Control refers to unedited cells. Each dot indicates an individual experiment. Donor = 5, n = 11. (C) Percentage of fetal hemoglobin (HbF) tetramer as measured by variant HPLC for HSPCs gene edited for PRR,  $\beta$ E1, and PRR- $\beta$ E1 and differentiated into erythroblasts. Donor = 3, n = 4. (D) Representative western blot image showing the band intensity of globin chains for erythroblasts derived from control, PRR,  $\beta$ E1, and PRR- $\beta$ E1 gene-edited HSPCs. The editing in PRR and  $\beta$ E1 indicates the percentage of indels by ICE analysis and for PRR- $\beta$ E1 edited, the percentage of editing includes the deletion + inversion quantified by ddPCR, cut site A and cut site B indels by ICE analysis. Donor = 1, n = 3. (E) Percentage of reticulocytes generated on erythroid differentiation of HSPCs gene edited for PRR,  $\beta$ E1, and PRR- $\beta$ E1. Flow cytometric analysis of reticulocytes percentage was quantified on day 20 of three-phase erythroid differentiation. Donor = 5, n = 11. (F) Ratio of erythroid (E) to granulocyte-monocyte (GM) CFU colonies. HSPCs were gene edited for AAVS1, PRR,  $\beta$ E1, and PRR- $\beta$ E1 and plated in methocult medium. Both BFU-E and CFU-E colonies were considered as erythroid (E) colonies. Donor = 2, n = 10. (G) Percentage of gene manipulation as measured by ddPCR for quantifying deletions in PRR- $\beta$ E1 and Sicilian HPFH. Indel analysis of AAVS1, BCL11A enhancer, and HBB promoter by ICE analysis. Donor = 2, n = 4. (H) FACS analysis of percentage of HbF<sup>+</sup>ve cells in erythroblasts generated from PRR- $\beta$ E1, Sicilian HPFH, BCL11A enhancer, and HBB promoter. Donor = 2, n = 4. (I) Representative hemoglobin variant HPLC chromatograms showing HbF and HbA tetramers in gene-edited cells. (J) Percentage of HbF tetramers. HSPCs were gene edited for PRR- $\beta$ E1, Sicilian HPFH, BCL11A enhancer, and HBB promoter, differentiated into erythroblasts and analyzed by variant HPLC. Donor = 2, n = 4. (K) Percentage of HbA tetramers. HSPCs were gene edited for PRR- $\beta$ E1, Sicilian HPFH, BCL11A enhancer, and HBB promoter, differentiated into erythroblasts and analyzed by variant HPLC. Donor = 2, n = 4. (L) Representative western blot image showing the band intensity of globin chains for erythroblasts derived from PRR- $\beta$ E1, Sicilian HPFH, BCL11A enhancer, and HBB promoter gene edited HSPCs. The editing in AAVS1, BCL11A enhancer, and HBB promoter indicates the indels quantified by ICE analysis. For PRR- $\beta$ E1 and Sicilian HPFH, editing indicates the percentage of deletion and inversion quantified by ddPCR excluding the cut site indels. Donor = 1, n = 2. Error bars represent mean  $\pm$  SEM, \*p  $\leq$  0.05, \*\*p  $\leq$  0.01, \*\*\*p  $\leq$  0.001, \*\*\*\*p  $\leq$  0.0001 (one-way ANOVA followed by Dunnett's multiple comparisons test).



(legend on next page)

PRR- $\beta$ E1 cells producing the highest proportion of HbF<sup>+</sup> cells (Figure 2H). PRR- $\beta$ E1-edited cells produced HbF tetramers that were 2-fold higher than the other targets and HbA tetramers were 3-fold lower (Figures 2I–2K). Western blot analysis further confirmed that PRR- $\beta$ E1 editing increased  $\gamma$ -globin chains and decreased  $\beta$ -globin chains relative to other targets tested (Figures 2L and S4H). The  $\gamma$ -globin levels in PRR- $\beta$ E1-edited cells were also higher in comparison with the HBB(-250)- $\beta$ E1 (Figure S4I).

### PRR- $\beta$ E1 gene-edited HSPCs repopulate for long-term and generate HbF<sup>+</sup> cells *in vivo*

To characterize the *in vivo* reconstitution capability of PRR- $\beta$ E1 gene-edited cells, we used NBSGW mice, which support robust human cell engraftment and erythropoiesis.<sup>27</sup> Gene editing was performed on HSPCs from two healthy donors using PRR- $\beta$ E1 and CRISPR RNA (crRNA) less RNP (control). The crRNA-free RNPs do not induce DNA double-strand breaks and therefore serve as an ideal control for assessing engraftment defects associated with Cas9 gene editing. The edited cells were transplanted into NBSGW mice as two cohorts, each infused with different donor cells and analyzed 16 weeks post transplantation.

The engraftment of PRR- $\beta$ E1-edited cells in the bone marrow, peripheral blood, and spleen of the mice was comparable with that of the control group (Figures 3A and S5A). The multilineage repopulation potential of engrafted cells was also comparable among the groups (Figure 3B). The percentage of CD235a<sup>+</sup> erythroblasts was also similar, confirming the intact erythropoiesis *in vivo* from PRR- $\beta$ E1-edited HSPCs. Importantly, genotyping of the long-term repopulating cells in all the mice revealed the retention of PRR- $\beta$ E1 editing, and the percentage of editing was comparable with that of infused cells in 12 of the 13 animals tested (Figure 3C). Next, human CD235a<sup>+</sup> erythroblasts were sorted from mouse bone marrow and were found to be increased in the proportion of HbF<sup>+</sup> cells *in vivo* following PRR- $\beta$ E1 editing (Figure 3D). Furthermore, *in vitro* erythroid differentiation of cells retrieved from mouse bone marrow showed a significant increase in HbF<sup>+</sup> cells (Figure 3E),  $\gamma/(\gamma+\beta)$  ratio (Figure 3F) and decreased  $\beta/(\gamma+\beta)$  ratio (Figure S5B) along with comparable reticulocyte production (Figure S5C).

To assess the serial repopulation potential of HSCs harboring PRR- $\beta$ E1 editing, we infused bone marrow cells of primary recipients (cohort 2) to secondary recipients and analyzed the bone marrow 14 weeks post infusion. The analysis showed similar frequencies of engraftment of PRR- $\beta$ E1-edited cells and control edited in the secondary recipients (Figure 3G).

### PRR- $\beta$ E1 gene editing without *ex vivo* culturing of HSPCs

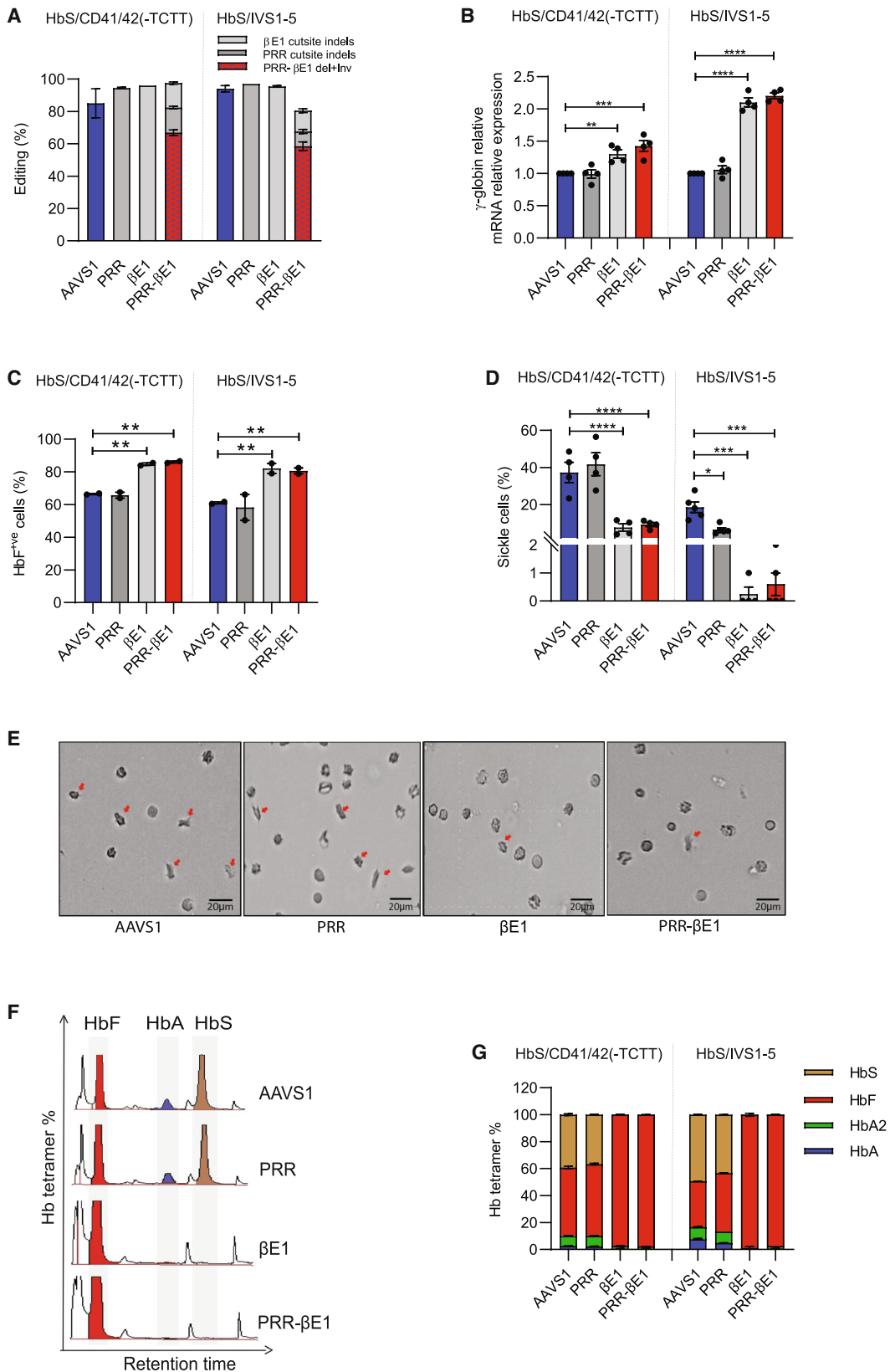
Unlike lentiviral transduction or HDR-based gene editing, cytokine pre-stimulation of HSPCs may not be necessary for NHEJ-mediated gene editing. To examine whether PRR- $\beta$ E1 gene editing is feasible without culture and cytokine pre-stimulation, HSPCs were electroporated immediately following purification and infused into NBSGW mice. The strategy was compared with the standard protocol, which consists of 48 h of cytokine stimulation prior to electroporation. On analysis after 16 weeks post transplantation, both groups exhibited comparable levels of bone marrow engraftment and PRR- $\beta$ E1 gene editing (Figures 3H and S5D). The multilineage repopulation potential of engrafted cells between the AAVS1 control and PRR- $\beta$ E1-edited cells remained comparable (Figure S5E). Functionally, PRR- $\beta$ E1-edited HSPCs from both uncultured and cultured HSPCs produced significantly more HbF<sup>+</sup> cells *in vivo* (Figure 3I), corroborating earlier findings. Furthermore, *in vitro* erythroid differentiation of cells from mouse bone marrow showed a significant increase in HbF<sup>+</sup> cells (Figure S5F) and  $\gamma/(\gamma+\beta)$  ratio (Figure 3J) and decreased  $\beta/(\gamma+\beta)$  ratio (Figure S5G) in PRR- $\beta$ E1-edited cells compared with the AAVS1 control.

### PRR- $\beta$ E1 gene-edited patient HSPCs reverse SCD phenotype

To test the potential of our PRR- $\beta$ E1 gene-editing strategy in the reversal of the sickle phenotype, the plerixafor-mobilized HSPCs from two SCD patients of compound heterozygous genotype HbS/CD41/CD42(-TCTT) and HbS/IVS1-5 (Figure S6A) were gene edited with Cas9-RNPs targeting AAVS1, PRR,  $\beta$ E1, and PRR- $\beta$ E1. The gene-editing frequency in each condition was >80%, with a PRR- $\beta$ E1 deletion frequency of >56% (Figure 4A). The gene-edited cells were *in vitro* differentiated into erythroblasts under hypoxia (5% O<sub>2</sub>)<sup>28</sup> and the erythroblasts derived from PRR- $\beta$ E1 and  $\beta$ E1 gene-edited HSPCs showed a significant increase in the  $\gamma$ -globin mRNA expression (Figure 4B) and the percentage of HbF<sup>+</sup> cells (Figure 4C).

### Figure 3. PRR- $\beta$ E1 gene-edited HSPCs repopulate for long-term and generate HbF<sup>+</sup> cells *in vivo*

Control and PRR- $\beta$ E1 gene-edited healthy donor HSPCs were transplanted into NBSGW mice and analyzed 16 weeks post transplantation (A–G). Each dot indicates a single mouse. Donor = 2. Each cohort indicates an independent experiment infused with HSPCs gene edited for PRR- $\beta$ E1. Error bars represent mean  $\pm$  SEM, ns, nonsignificant. \*\*\*p  $\leq$  0.001, \*\*\*\*p  $\leq$  0.0001 (two-way ANOVA followed by Dunnett's test). (A) Percentage of engraftment in the bone marrow, peripheral blood, and spleen calculated flow cytometrically using hCD45 and mCD45.1 markers. (B) Percentage of HSPC and lineage markers in bone marrow (BM) – CD3 (T cells), CD13 (monocyte), CD19 (B cells), CD235a (erythroid), and CD34 (HSPCs) in engrafted cells. CD235a<sup>+</sup> cells were analyzed from CD45<sup>+</sup> cells. (C) Percentage of PRR- $\beta$ E1 deletion+inversion (Del+Inv), PRR cut site indels, and  $\beta$ E1 cut site indels in PRR- $\beta$ E1 gene-edited HSPCs in infused fraction and in engrafted cells. (D) Percentage of HbF<sup>+</sup> cells in hCD235a<sup>+</sup> cells obtained from mouse BM. (E) Percentage of HbF<sup>+</sup> cells generated by erythroid differentiation of engrafted cells in the BM. (F) Ratio of  $\gamma/(\gamma+\beta)$  chains. Mouse BM was collected, *in vitro* differentiated into erythroblasts and analyzed by chain HPLC. (G) Percentage of engraftment in BM of secondary recipients analyzed 14 weeks post transplantation. AAVS1 and PRR- $\beta$ E1 gene-edited healthy donor HSPCs were gene edited immediately after CD34 purification (day 0) and 48 h post CD34 purification (day 2) and transplanted into NBSGW mice and analyzed 16 weeks post transplantation (G)–(J). Each dot indicates a single mouse. Donor = 1. Error bars represent mean  $\pm$  SEM, ns, nonsignificant. \*p  $\leq$  0.05 (two-way ANOVA followed by Dunnett's test). (H) Percentage of PRR- $\beta$ E1 deletion+inversion (Del+Inv), PRR cut site indels, and  $\beta$ E1 cut site indels in PRR- $\beta$ E1 gene-edited HSPCs in Day 0 and Day 2 edited input fraction and in engrafted cells. (I) Percentage of HbF<sup>+</sup> cells in hCD235a<sup>+</sup> cells obtained from mouse BM. (J) Ratio of  $\gamma/(\gamma+\beta)$  chains. Mouse BM was collected, *in vitro* differentiated into erythroblasts, and analyzed by chain HPLC.



(legend on next page)



Further, we performed a sickling assay by treating reticulocytes with sodium metabisulfite. Upon treatment, control and PRR edited cells underwent sickling, whereas the  $\beta$ E1 and PRR- $\beta$ E1-edited groups had a 12-fold (HbS/CD41/CD42(-TCTT)) and 30-fold (HbS/IVS1-5) reduction in sickling, respectively (Figures 4D and 4E). Variant HPLC analysis further showed that all the hemoglobin in the  $\beta$ E1 and PRR- $\beta$ E1-edited cells was composed of HbF tetramers with nearly complete reduction of HbS (Figures 4F and 4G).

#### PRR- $\beta$ E1 gene-edited patient HSPCs reverse $\beta$ -thalassemia phenotype

To test the therapeutic potential of our gene-editing strategy in reversing  $\beta$ -thalassemia defects, we edited HSPCs obtained from  $\beta$ -thalassemia patients of three different  $\beta^0/\beta^0$  genotypes: CD26 (G>A)/IVS1-5 (G>C), IVS1-5 (G>C), and CD30 (G>A) (Figure S6B). These  $\beta$ -thalassemia mutations are highly prevalent in India and Southeast Asian countries.<sup>29,30</sup> Due to poor peripheral blood mononuclear cell (PBMNC) yield, CD26 (G>A)/IVS1-5 (G>C) PBMNCs were differentiated into erythroblasts and edited on day 8 of erythroid differentiation. The PRR- $\beta$ E1 gene-editing efficiency remained >80% in all the genotypes (Figure 5A). In *in vitro* erythropoiesis,  $\beta$ E1 and PRR- $\beta$ E1 cells showed a significant increase in the frequency of HbF<sup>+</sup> cells (Figure S7A) and  $\gamma/(\gamma+\beta)$  ratio (Figure S7B) and decrease in  $\beta/(\gamma+\beta)$  ratio (Figure S7C). The ratio of  $\alpha$  to non- $\alpha$ -globin chains was also observed to be reduced (Figures 5B and 5C), suggesting the reduction of free  $\alpha$ -globin chains. Western blot analysis of CD30 (G>A) gene-edited cells further confirmed that PRR- $\beta$ E1 editing resulted in enhanced induction of  $\gamma$ -globin chains (Figures 5D and S7D).

Ineffective erythropoiesis, the classical phenotype of  $\beta$ -thalassemia, results from increased reactive oxygen species (ROS) levels, apoptosis of erythroid progenitors, and reticulocyte maturation arrest.<sup>4,31</sup> Erythroblasts originated from the PRR- $\beta$ E1 gene-edited group showed a modest decrease in ROS levels (Figure S7E), a decrease in the proportion of apoptotic erythroblasts (stained by Annexin V) (Figures 5E and 5F), and importantly, a 3-fold increase in reticulocyte generation (Figures 5G and 5H) compared with the control. All these findings suggest that PRR- $\beta$ E1 gene editing functionally rescues erythropoiesis in  $\beta$ -thalassemia by robust activation of  $\gamma$ -globin and silencing of defective  $\beta$ -globin (Figure S9).

#### PRR- $\beta$ E1 gene-edited HSPCs have intact genome integrity

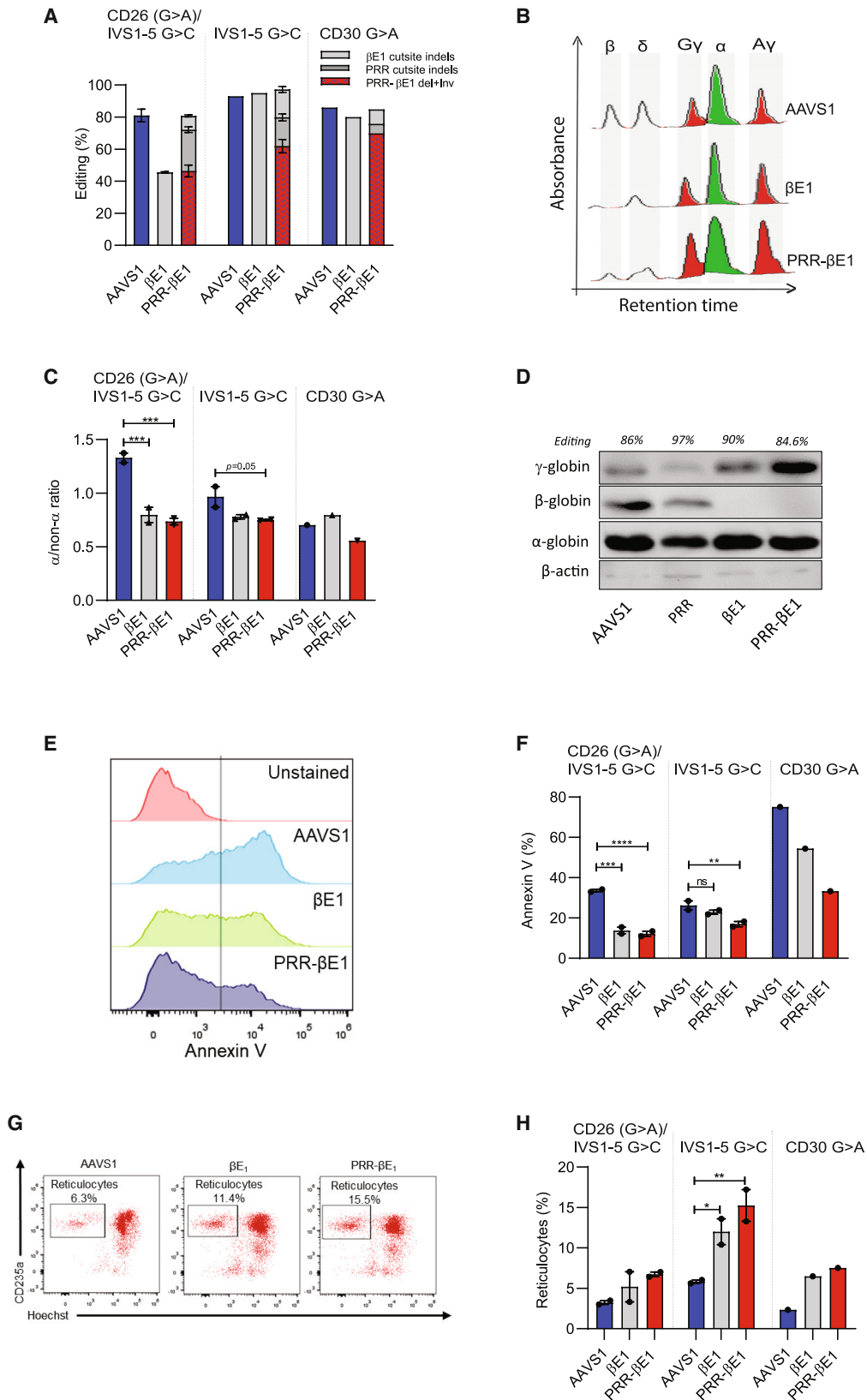
Reportedly, Cas9-generated DNA double-strand breaks pose a risk of genome-wide effects, such as genomic rearrangements.<sup>32,33</sup> Using HSPCs with micronuclei as a readout for cells with genomic instability, we microscopically evaluated individual HSPCs. In these experiments, we edited HSPCs using HiFi-Cas9, which has been demonstrated to minimize off-target editing and off-target mediated translocation.<sup>33,34</sup> HiFi-Cas9 retained the same frequency of on-target gene editing obtained in our earlier experiments with wild-type Cas9 (Figure 6A). Mitomycin C, an interstrand crosslinker that induces chromosomal rearrangements, was used as positive control. The frequency of micronuclei-positive HSPCs in PRR- $\beta$ E1-edited HSPCs was not significantly greater than in unedited control HSPCs (Figure 6B).

As a second method, we employed array-based KaryoStat analysis to identify chromosomal abnormalities. The edited HSPCs were expanded for 7 days to magnify any potential defect. The whole-genome coverage analysis with a resolution of >1 Mb revealed that the PRR- $\beta$ E1 gene-edited HSPCs exhibited neither loss nor gain of chromosomal copy number (Figure 6C).

To analyze genomic integrity with the highest resolution possible, we performed chromosomal aberrations analysis by single-targeted ligation-mediated PCR sequencing (CAST-Seq), which is sensitive enough to detect a single translocation event in 10,000 cells and can classify the type of structural variation.<sup>33</sup> CAST-Seq detects chromosomal abnormalities caused by on-target editing as well as the fusion of off-target edited sites to the on-target region. Upon gene editing HSPCs with HiFi-Cas9, CAST-Seq identified a single off-target-mediated translocation event between chr16: 684705–685217, which codes for the 3'- untranslated region (UTR) of WD repeat domain 24 (WDR24), and the on-target site (Figure 6D). This translocation was identified in two of our four CAST-Seq runs. The number of unique footprints (CAST-Seq hits), which testify to this translocation, is very low (13 hits) compared with the cumulated 58,897 on-target hits. This indicates that this particular translocation is an ultra-rare event, happening at a frequency close to the lower limit of detection of CAST-Seq (i.e., 0.01%). No homology-mediated translocation events were identified in the modified HSPCs. All these experiments indicate that chromosomal abnormalities occurred at very low frequency and the PRR- $\beta$ E1 gene editing does not majorly compromise the integrity of the genome.

#### Figure 4. PRR- $\beta$ E1 gene-edited patient HSPCs reverses sickle cell disease phenotype

Plerixafor-mobilized HSPCs from sickle cell patients of genotype HbS/CD41/42(-TCTT) and HbS/IVS1-5 were gene edited for AAVS1, PRR,  $\beta$ E1, and PRR- $\beta$ E1. Error bars represent mean  $\pm$  SEM. \* $p \leq 0.05$ , \*\* $p \leq 0.01$ , \*\*\* $p \leq 0.001$ , \*\*\*\* $p \leq 0.0001$  (two-way ANOVA followed by Dunnett's test). (A) Percentage of gene editing. Indels measured by Sanger sequencing and ICE analysis. Deletion/inversion (Del+Inv) (red checker box) in PRR- $\beta$ E1 quantified by ddPCR. The indels in the PRR- $\beta$ E1 edited cells (gray checker box) were assessed using ICE analysis. Donor = 2, n = 4. (B) Relative globin mRNA expression. The patient HSPCs were gene edited for PRR,  $\beta$ E1, and PRR- $\beta$ E1 and differentiated into erythroblasts. Real-time PCR analysis was used for mRNA quantification and the globin chain expression was normalized with  $\beta$ -actin. The patient genotype is indicated at the bottom. Donor = 2, n = 4. (C) Percentage of HbF<sup>+</sup> cells. The gene-edited patient HSPCs were differentiated into erythroblasts and intracellular HbF positive cells were analyzed by FACS. Donor = 2, n = 4. (D) Percentage of sickle cells. Gene-edited patient HSPCs were differentiated into erythroblasts in hypoxia (5% O<sub>2</sub>) and the FACS sorted reticulocytes were treated with 1.5% sodium metabisulfite. Cells were scored from random fields using EVOS FL Auto Imaging System microscope. At least eight fields were analyzed. Each field contained a minimum of 150 cells. Donor = 2, n = 4. (E) Representative image of sickle cells (red arrow) and non-sickled cells. (F) Representative variant HPLC chromatogram showing HbA, HbF, and HbS. Donor = 2, n = 4. (G) Proportion of hemoglobin tetramer. The gene-edited patient HSPCs were differentiated into erythroblasts and the hemoglobin tetramers were analyzed by variant HPLC. Donor = 2, n = 4.



(legend on next page)

### PRR- $\beta$ E1 gene editing reconfigures chromosome looping and alters globin expression

Long-range chromatin interaction of the locus control region (LCR) and the promoters in the  $\beta$ -globin cluster regulate developmental stage-specific expression of globin genes.<sup>35</sup> To test the potential impact of PRR- $\beta$ E1 gene editing on the configuration of the  $\beta$ -globin cluster, we employed a circular chromosome conformation capture (4C) assay. An interaction between hypersensitive site 1 (HS1) within the LCR and the *HBG2* promoter was observed in HUDEP-2 control cells. However, this interaction was enhanced in HUDEP-2 clones harboring a PRR- $\beta$ E1 biallelic deletion. Furthermore, the interaction between other HS sites and *HBG2* promoters was newly gained in PRR- $\beta$ E1 deleted cells. (Figure 7A). These data suggests that genomic proximity between the LCR and the *HBG* gene increases upon PRR- $\beta$ E1 deletions and thus reactivates  $\gamma$ -globin in edited cells.

Thereafter, to understand the *trans*-acting factors involved in  $\beta$ -globin reactivation in the PRR- $\beta$ E1 gene-edited cells, transcriptome analysis was carried out using the erythroblasts generated *in vitro* from gene-edited HSPCs. This analysis confirmed the overexpression of *HBG1* and *HBG2* with simultaneous downregulation of *HBB*. *HBG* was not among the top 20 significantly upregulated candidates in  $\beta$ E1 and showed a distinct set of upregulated genes than PRR- $\beta$ E1 (Figure 7B and S8A). This indicates that different pathways are involved in PRR- $\beta$ E1 and  $\beta$ E1 editing for  $\gamma$ -globin activation, with  $\beta$ E1 editing resulting in a weaker level of  $\gamma$ -activation on comparison. Cluster per million (cpm) values for the globin transcripts obtained from RNA sequencing further support higher  $\gamma$ -globin induction on PRR- $\beta$ E1 editing (Figure 7C).

The transcriptome analysis and the followed-up real-time PCR analysis indicated the overexpression of *HBBP1* in PRR- $\beta$ E1 gene-edited cells (Figure 7D). *HBBP1* was recently implicated in  $\gamma$ -globin activation.<sup>36</sup> *BGLT-3*, which is reported to promote transcriptional assembly at the  $\gamma$ -globin promoter, was seen to be abundant in edited cells by RT-PCR (Figure 7E).<sup>37</sup> Our gene set enrichment analysis (GSEA) with the published gene sets for HPFH mutation<sup>38</sup> showed a high normalized enrichment score (NES) of 2.13 for PRR- $\beta$ E1 gene-edited cells confirming that PRR- $\beta$ E1 gene editing creates an HPFH phenotype (Figure S8B), whereas the  $\beta$ E1 gene-edited cells showed relatively weaker enrichment (NES = 1.5) (Figure S8C).

All these findings suggest that the  $\gamma$ -globin activation in PRR- $\beta$ E1 gene-edited cells occurs through altered chromatin looping mediated by promoter competition for the LCR and is similar to the HPFH phenotype.

### DISCUSSION

Genetic reactivation of developmentally silenced HbF has gained considerable attention as a potential therapy for the broad spectrum of  $\beta$ -hemoglobinopathies. In this study, we have identified the PRR- $\beta$ E1 sequence as a core HbF regulatory region present in all the deletional HPFH mutations. When present, PRR- $\beta$ E1 effectively reverses the cellular phenotype of both SCD and  $\beta$ -thalassemia major by disrupting the production of defective  $\beta$ -globin and concurrently inducing robust HbF production through LCR switching mechanism. We specifically showed that PRR- $\beta$ E1 gene-edited HSPCs have sustained engraftment, repopulation fitness, and genome integrity, highlighting the potential of this approach for future clinical studies.

Among the naturally existing mutations that produce pancellular HbF, deletional HPFH mutations are highly prevalent and are shown to generate a high frequency of HbF<sup>+ve</sup> RBCs.<sup>13</sup> Even a heterozygous deletion can result in an HbF level of 65.6% with 8.9 g/dL of hemoglobin on co-inheritance with  $\beta$ -thalassemia.<sup>21</sup> Identifying the core region in HPFH deletions will enable us to recreate the HPFH phenotype by gene editing only the core region. The PRR region is conserved in  $\delta\beta$ -thalassemia but excised in HPFH deletions.<sup>39</sup> However, deletion of the PRR site alone did not activate the HbF in our studies, consistent with earlier observations.<sup>39</sup> Even a deletion of 10.5 kb spanning the PRR region to the region located before the  $\beta$ -globin promoter had little effect on  $\gamma$ -globin production. In contrast, disruption of  $\beta$ E1 alone induced  $\gamma$ -globin production. Shen et al. showed that the improved  $\gamma$ -globin levels obtained by disrupting the *HBB* gene and its regulatory region is not sufficient to compensate for the loss of  $\beta$ -globin.<sup>40</sup> Our results provide compelling evidence that simultaneous disruption of the PRR region and  $\beta$ -globin reactivates  $\gamma$ -globin robustly without negatively impacting the erythroid maturation. While PRR disruption ensures that  $\delta\beta$ -thalassemia-like phenotype is not created and the  $\beta$ E1 cut site confirms that even in the case of inversion or indels, the  $\beta$ -globin gene expression gets ablated and is associated with  $\gamma$ -globin production: thus PRR- $\beta$ E1 is a more potent target than the original Sicilian HPFH.

### Figure 5. PRR- $\beta$ E1 gene-edited patient HSPCs reverse $\beta$ -thalassemia phenotype

The G-CSF mobilized HSPCs from  $\beta$ -thalassemia patients of genotype IVS1-5 (G>C), and CD30 (G>A) were gene edited for AAVS1,  $\beta$ E1, and PRR- $\beta$ E1. For HbE (G>A)/IVS1-5 (G>C), the PBMCs were differentiated into erythroblasts and gene edited for AAVS1,  $\beta$ E1, and PRR- $\beta$ E1. Error bars represent mean  $\pm$  SEM. \* $p \leq 0.05$ , \*\* $p \leq 0.01$ , \*\*\* $p \leq 0.001$  (two-way ANOVA followed by Dunnett's test). Donor = 3, n = 5. (A) Percentage of gene editing in HSPCs. Deletion/Inversion (Del+Inv) in PRR- $\beta$ E1 as quantified by ddPCR. Indels of the cut sites PRR and  $\beta$ E1 were measured by ICE analysis. (B) Representative globin chain HPLC chromatograms. (C)  $\alpha$ /non- $\alpha$  ratio in the erythroblasts generated from gene-edited HSPCs. (D) Representative western blot image showing the band intensity of globin chain erythroblasts derived from AAVS1, PRR,  $\beta$ E1, and PRR- $\beta$ E1 gene-edited CD30 (G>A) patient HSPCs. Donor = 1, n = 1. The editing in PRR and  $\beta$ E1 indicates the percentage of indels in ICE analysis and for PRR- $\beta$ E1 edited, the percentage of editing includes the deletion + inversion quantified by ddPCR, cut site A and cut site B indels by ICE analysis. Donor = 1, n = 1. (E) Representative flow cytometry image of Annexin V staining. (F) Percentage of Annexin V in the erythroblasts generated from gene-edited HSPCs. (G) Representative flow cytometry plots of reticulocytes marked by CD235a<sup>+</sup>/Hoechst<sup>-</sup>. (H) Percentage of reticulocytes generated from gene-edited HSPCs.

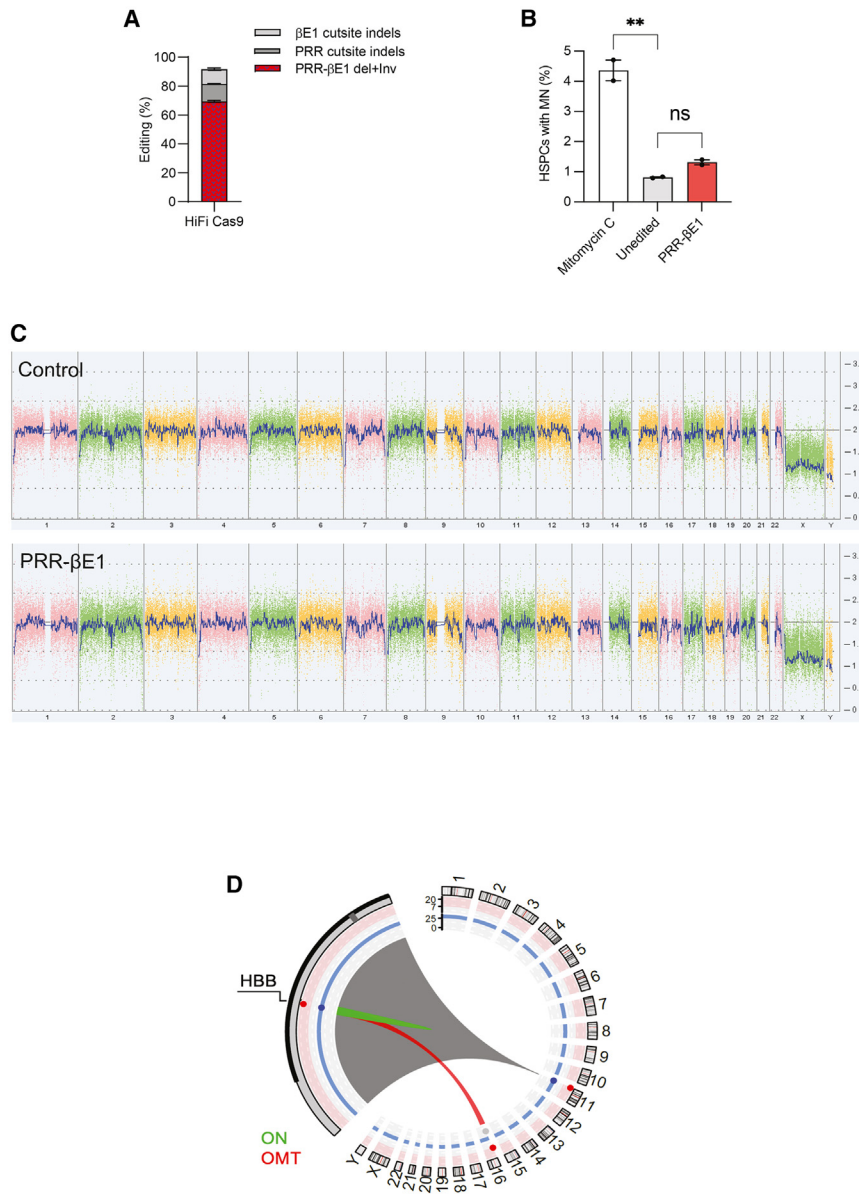


**Figure 6. PRR-βE1 gene-edited HSPCs have intact genome integrity**

(A) Percentage of gene editing on PRR-βE1 editing in healthy donor HSPCs using HiFi Cas9. Indels measured by Sanger sequencing and ICE analysis. Deletion/inversion (Del+Inv) (red checker box) in PRR-βE1 quantified by ddPCR. Donor = 1, n = 2. (B) Percentage of micronucleus (MN) in Mitomycin C treated, unedited, and PRR-βE1 gene-edited HSPCs scored 48 h post nucleofection after staining with Giemsa. Donor = 1, n = 2. (C) KaryoStat analysis of healthy donor HSPCs gene edited for PRR-βE1 deletion. Donor = 1, n = 2. (D) Circos plot showing off-target mediated translocation between the PRR-βE1 on-target site and βE1 off-target site in PRR-βE1 edited samples present in chr16 identified by CAST-Seq. Donor = 1, n = 4. Error bars represent mean ± SEM. ns, nonsignificant, \*\*p ≤ 0.01 (one-way ANOVA followed by Dunnett's multiple comparisons test).

and the region resembles British black and Croatian β-thalassemia genotypes.<sup>24,25</sup> βE1 gene-editing also disrupts the β-globin and reactivates the γ-globin, supporting the earlier findings.<sup>19,41</sup> The loss of β-globin reduces the levels of ATF4, which in turn decreases MYB and BCL11A to upregulate γ-globin.<sup>41</sup> This approach also resulted in decreased γ-globin activation than PRR-βE1 editing (Figures 2D, 5D, and 7C). Secondly, through a single-cell functional assay, Shen et al. demonstrated globin chain imbalance in erythroid colonies with β-globin (*HBB-HBD*<sup>-/-</sup>) disruption but not in colonies with an *HBB-3.5kb* deletion that encompasses the PRR 3.5kb region, HBD, and HBB.<sup>40</sup> A long-range distal regulatory role has been proposed for the region upstream of HBD and this merges with the functional role of BCL11A in the HbF reactivation.<sup>40</sup>

Ramdiar et al. reported a strategy of combining lentiviral transduction of anti-sickling β-globin and gene editing to disrupt endogenous β-globin, and enhance the proportion of anti-sickling hemoglobin.<sup>42</sup> This clearly depicts the competition between defective endogenous β-globin chains and exogenously supplemented globin chains for hemoglobin tetramer formation. In the ongoing clinical trial CLIMB SCD-121, HSPCs from SCD patients were gene edited for the BCL11A erythroid-specific enhancer; the gene-editing efficiency was up to 82.6%. HbF levels were 43.2% and the presence of HbS tetramers was up to 52.3%.<sup>12</sup> This indicates that, irrespective of the gene-editing efficiency and γ-globin activation efficacy, an intact β-globin regulatory region allows production of mutated β-globin chains at reduced levels. Similarly, in the BCL11A shRNA clinical trial, HbS constitutes up to 70% of hemoglobin tetramers.<sup>11</sup> The PRR-βE1-editing strategy directly excises the promoter and coding regions of β-globin, resulting in a major

We observed a new genomic interaction between *HBB2* and a region downstream of *HBB* in PRR-βE1-edited cells (Figure 7A). Interestingly, this interaction site is deleted in Sicilian HPFH. Whether this region has a regulatory role on *HBB* expression and contributes to increased HbF in PRR-βE1 over Sicilian HPFH is to be explored.

While our manuscript was under preparation, two new articles provided deeper insight into the PRR-βE1 regulatory region. Topfer et al. analyzed both HPFH and δβ-thalassemia deletions and identified that the disruption of the β-globin promoter is sufficient for HbF reactivation.<sup>19</sup> One of our initial targets for editing, *HBB(-250)-βE1*, editing closely mimics the target analyzed by Topfer et al., and it had relatively less γ-globin activation over PRR-βE1 editing in our study (Figure S4I),

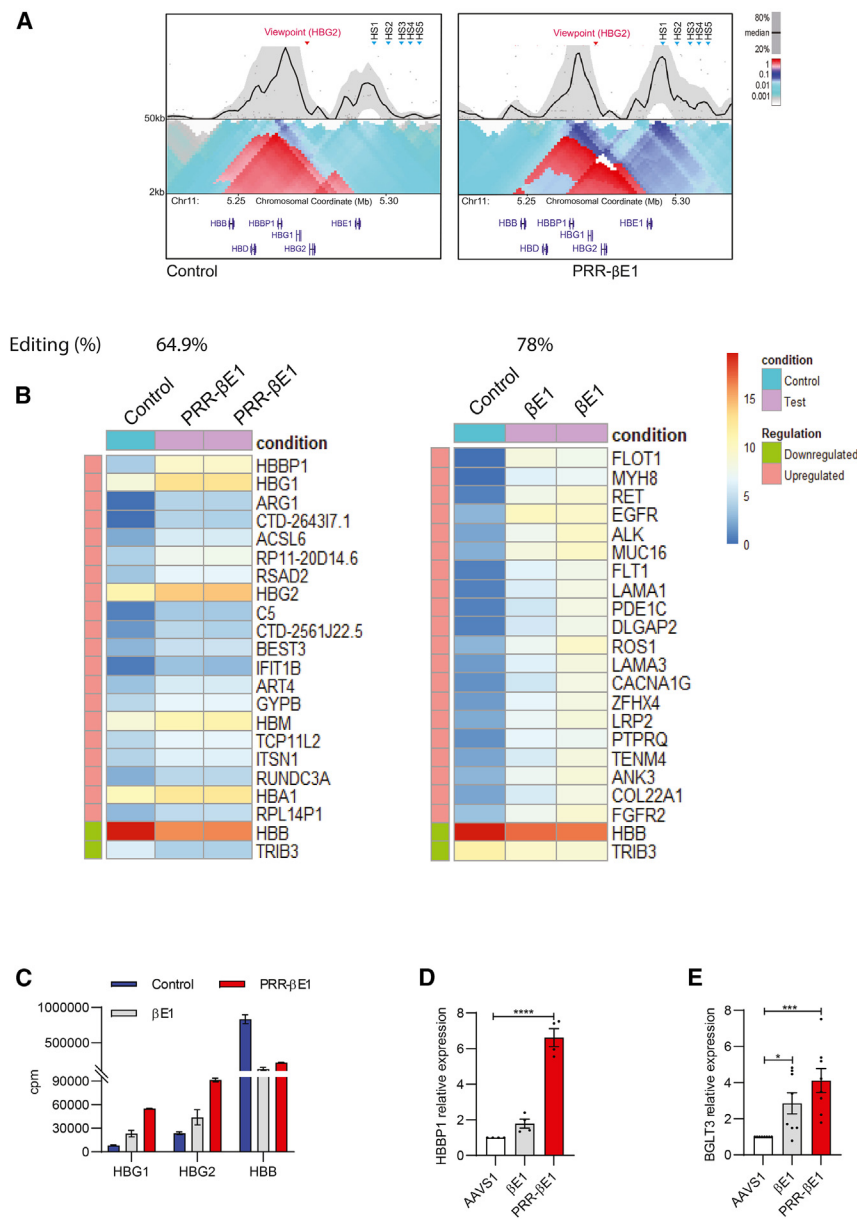


**Figure 7. PRR-βE1 gene editing reconfigures chromosome looping and alters globin expression**

(A) 4C analysis of single-cell sorted control and two PRR-βE1 biallelic gene-edited HUDEP-2 clones using *HBG2* promoter as a viewpoint.  $n = 4$ . (B) Heatmap of the top differentially expressed genes of erythroblasts derived from PRR-βE1 and βE1 gene-edited HSPC indicating the relative gene expression pattern of genes up- and downregulated compared with control. Donor = 1,  $n = 2$ . (C) Cluster per million (cpm) values for the globin transcripts obtained from RNA sequencing. (D) Relative HBBP1 mRNA expression in erythroblasts derived from βE1 and PRR-βE1 gene-edited HSPCs compared with AAVS1. The globin chain expression is normalized with β-actin. Donor = 1,  $n = 4$ . (E) Relative BGLT3 mRNA expression in erythroblasts derived from βE1, a PRR-βE1 gene-edited HSPC compared with AAVS1. The globin chain expression is normalized with β-actin. Donor = 2,  $n = 8$ . Error bars represent mean  $\pm$  SEM.

incompetent.<sup>26,43</sup> To our knowledge, this is the first study to demonstrate that HSPCs with large deletions can engraft and repopulate in both primary and secondary recipients. Our study also suggests that gene editing for large HPFH deletions is feasible without chromosomal aberrations when HiFi-Cas9 is used in conjunction with a carefully chosen single guide RNA (sgRNA). The gene-editing approach and the cytokine pre-stimulation that we described can potentially simplify the manufacturing process and reduce the cost associated with HSPC gene therapy.

In conclusion, our study sheds light on the crucial function of the PRR-βE1 region in regulating HbF and shows that this region is a key target for gene editing to activate fetal hemoglobin robustly to reduce mutated β-globin and to reverse major β-hemoglobinopathies phenotype.

This study provides the first proof that large genomic sequences can be precisely modified in the HSPCs without endangering the multilineage repopulation potential and genome integrity.

## MATERIALS AND METHODS

### Purification and culture of CD34<sup>+</sup>ve HSPCs

The unused G-CSF mobilized peripheral blood collected for allogeneic stem cell transplantation and Plerixafor-mobilized peripheral blood from SCD, or β-thalassemia patients were collected from transplantation unit of Christian Medical College, Vellore with prior institutional review board approval. The CD34<sup>+</sup>ve HSPCs were purified as described in our previous studies.<sup>44–46</sup>

reduction in the concentration of HbS, which will prevent the sickling of RBCs. This strategy will also be applicable for β-thalassemia, where the intact β-globin promoter drives production of truncated β-globin chains (Figure S9). Whether such an approach results in any free alpha globin levels is yet to be determined.

For a while, HPFH deletions were considered to be potential gene-editing targets. However, there were no reports on the genome integrity of the HSPCs and their ability to engraft post editing. HSPCs with a 4.9-kb deletion in the *HBG* promoter were shown to be lost post transplantation, and it was hypothesized that HSPCs having larger deletions are transplantation

### Electroporation of RNP complex in HUDEP-2, CD34<sup>+</sup>ve cells and $\beta$ -hemoglobinopathies patient HSPCs

SgRNAs were designed using CRISPR Design Tool (Synthego) and CRISPR-Cas9 guide RNA design checker (IDT), and the efficient gRNAs with least off-target sites were selected. List of gRNA used in the study is mentioned in Table S2. For nucleofection of HUDEP-2 cell lines, 100 pmol of Cas9 (Takara) was incubated at room temperature for 10 min with 200 pmol of sgRNA (Synthego). For dual sgRNA gene editing, 100 pmol of Cas9 RNP with cut site A sgRNA and 100 pmol of Cas9 RNP with cut site B sgRNA were nucleofected (Lonza 4D nucleofector) with CA137 pulse code. For electroporation of CD34<sup>+</sup>ve HSPCs, 50 pmol of Cas9 RNP with sgRNA against PRR and 50 pmol of Cas9 RNP with sgRNA against  $\beta$ E1 were used;  $2 \times 10^5$  cells were electroporated using P3 primary cell solution and supplement and were electroporated using Lonza 4D nucleofector with DZ100 pulse code.

For nucleofection of SCD and  $\beta$ -thalassemia patient HSPCs, 100 pmol of Cas9 (Takara) was incubated at room temperature for 10 min with 200 pmol of sgRNA (Synthego). For dual sgRNA gene editing 100 pmol of Cas9 RNP with cut site A sgRNA and 100 pmol of Cas9 RNP with cut site B sgRNA were nucleofected (Lonza 4D nucleofector) with DZ100 pulse code.

### HUDEP-2 expansion and differentiation

The HUDEP-2 cells were cultured in StemSpan SFEM-II media containing SCF (50 ng/mL), EPO (3 U/mL), dexamethasone (1  $\mu$ M), doxycycline (1  $\mu$ g/mL), and glutamine (1x) at  $2 \times 10^5$  cells/mL confluency with media change on alternative days. For erythroid differentiation, previously reported protocol with minor modifications was used.<sup>47</sup> The cells were seeded at a density of  $2 \times 10^5$  cells/mL in IMDM GlutaMAX Supplement media containing 3% AB serum, 2% FBS, insulin (10  $\mu$ g/mL), heparin (3U/mL), EPO (3U/mL), Holotransferrin (200  $\mu$ g/mL), SCF (100 ng/mL), interleukin (IL)3 (10 ng/mL) and doxycycline (1  $\mu$ g/mL). On day 2, cells were seeded at a cell density of  $3.5 \times 10^5$  cells/mL. On day 4, the cells were seeded at a cell density of  $5 \times 10^5$  cells/mL in the media containing the above-mentioned cytokine except doxycycline. On day 6, the cells were seeded at a cell density of  $1 \times 10^6$  cells/mL in the media with all the components of day 4 media along with increased concentration of Holotransferrin (500  $\mu$ g/mL). The cells were analyzed for HbF<sup>+</sup>ve cells, differentiation profile, and globin chains using HPLC.

### Erythroid differentiation of CD34<sup>+</sup>ve HSPCs

The protocol for erythroid differentiation from CD34<sup>+</sup>ve HSPCs was adopted from the literature with minor modifications.<sup>48</sup> The three-phase erythroid differentiation protocol involves culturing the CD34<sup>+</sup>ve cells at a seeding density of  $5 \times 10^4$  cells/mL in phase I from day 0 to day 8 with a media change on day 4. The phase I media is prepared using IMDM GlutaMAX Supplement media containing 5% AB serum, insulin (20  $\mu$ g/mL), heparin (2 U/mL), EPO (3 U/mL), Holotransferrin (330  $\mu$ g/mL), SCF (100 ng/mL), IL3 (50 ng/mL) and hydrocortisone (1  $\mu$ g/mL). In phase II, the cells were seeded at a density of  $2 \times 10^5$  cells from day 8 to day 12 in media containing

all the components of phase I except hydrocortisone and IL3. In phase III, the cells were seeded at a density of  $5 \times 10^5$  cells from day 12 to day 20 in media containing all the components of phase II except SCF with a media change on day 16. On day 20, the cells were collected for F<sup>+</sup>ve cells analysis, differentiation marker analysis, and for hemoglobin and globin chain HPLC.

For differentiation of healthy donor and thalassemia patient HSPCs, the cells were cultured at 37°C, 5% CO<sub>2</sub> and in normoxia conditions (21% O<sub>2</sub>). For the erythroid differentiation of SCD patient HSPCs, the above protocol was followed except the oxygen levels where we have cultured the SCD patient cells under hypoxic conditions (5% O<sub>2</sub>) until day 20 to promote robust sickling of the erythroid differentiated cells.<sup>28</sup>

### Flow cytometry

For HbF<sup>+</sup>ve cell analysis,  $1 \times 10^5$  erythroid differentiated cells were briefly washed with PBS and fixed with 0.05% glutaraldehyde for 10 min and permeabilized with 0.1% Triton X-100 for 5 min. The cells were stained with anti-HbF APC antibody (dilution 1:50) and were acquired and analyzed using Cytoflex LX Flow Cytometer (Beckmann Coulter) or AriaIII flow cytometer (BD Biosciences) and analyzed using FlowJo (BD Biosciences). For erythroid differentiation analysis,  $1 \times 10^5$  cells from the terminal day of erythroid differentiation were stained for erythroid differentiation markers anti-CD71-FITC (dilution 1:33), anti-CD235a PE-Cy7 (dilution 1:50) and Hoechst 33342 (dilution 1:1,000). After 20 min of incubation in the dark, the cells were washed with PBS followed by analysis using Cytoflex LX Flow Cytometer (Beckmann Coulter) or AriaIII flow cytometer (BD Biosciences).

### In vivo engraftment analysis

All the *in vivo* experiments in NBSGW mice models were conducted with approval from IAEC of Christian Medical College, Vellore, India. The NBSGW mice were bred in-house and were conditioned with busulfan at a concentration of 12.5 mg/kg of body weight, 48 h prior to the infusion.

CD34<sup>+</sup> HSPCs were pre-stimulated for 36 to 40 h with culture media containing appropriate cytokines and RUS cocktail<sup>44,45</sup>;  $5 \times 10^5$  to  $6 \times 10^5$  cells of control edited and PRR- $\beta$ E1 edited were infused into NBSGW mice, immediately post electroporation. Sixteen to 18 weeks post infusion, the mice were euthanized and peripheral blood, bone marrow, and spleen were collected. After RBC lysis buffer incubation, the harvested cells were incubated with mouse Fc block and stained with hCD45 and mCD45 antibody. The % of engraftment is calculated using the formula (% hCD45/% hCD45 + % mCD45)  $\times$  100. In addition, the multilineage markers including CD19, CD3, CD13, and CD235a in bone marrow hCD45+ cells were also analyzed. For *ex vivo* erythroid differentiation,  $3 \times 10^6$  cells were harvested from mouse bone marrow, seeded in erythroid differentiation media, and at the end of phase III of differentiation, the % of F<sup>+</sup>ve cells, the differentiation profile, and globin chains were analyzed. For *in vivo* HbF<sup>+</sup>ve cell analysis in NBSGW,  $1 \times 10^6$  bone marrow cells

were stained with 10  $\mu\text{L}$  of CD235a antibody and sorted based on the presence of immunophenotypic marker CD235a, followed by  $F^{+ve}$  cell analysis. For secondary infusion,  $4 \times 10^6$  cells from the pooled fraction harvested from primary recipient bone marrow were infused to secondary recipients 48 h post busulfan conditioning. After 14 weeks, the mice were euthanized and the harvested cells were stained with hCD45 and mCD45 antibody for calculating the % of engraftment.

#### **In vitro sickling assay**

Sickling assay protocol was adopted from the literature with minor modifications.<sup>28,49</sup> The gene-edited SCD patient HSPCs were differentiated until day 20 of erythroid differentiation under hypoxia (5%  $\text{O}_2$ ). On day 20 of erythroid differentiation, enucleated cells (reticulocytes) marked by Hoechst<sup>-ve</sup> were flow sorted. The flow sorted cells were resuspended with phase III erythroid differentiation medium and seeded in 24-well plates. Freshly prepared 1.5% sodium metabisulfite in 1x PBS were mixed with phase III media containing the reticulocytes in 1:1 ratio and incubated at 37°C for 1 h under hypoxia (5%  $\text{O}_2$ ). After the incubation, the sides of the 24-well plate were covered with parafilm. Live cell images were acquired using EVOS FL Auto microscope. The percentage of sickle cells were calculated as number of sickle cells divided by the total number of cells.

#### **Quantitative real-time PCR analysis**

A total of  $3 \times 10^6$  cells from the day 8 of CD34<sup>+</sup> HSPC and day 6 of HUDEP-2 erythroid differentiation were used for total RNA using an RNeasy Mini Kit (Qiagen). For reverse transcription using PrimeScript RT reagent kit (Takara Bio Inc.), 1  $\mu\text{g}$  of extracted RNA was used according to the manufacturer's instructions. For quantitative PCR, the SYBR Premix Ex Taq II (Takara Bio) was used for quantifying the specific transcripts and analyzed with QuantStudio 6 Flex (Life Technologies). Primers used in qPCR analysis are mentioned in Table S5.

#### **Colony formation assay**

Forty-eight hours post electroporation,  $5 \times 10^2$  HSPCs were seeded in 1.5 mL of Methocult Optimum (STEMCELL Technologies), and after 14 days, the colonies were scored based on the morphology as CFU-GM, CFU-GEMM, BFU-E, and CFU-E.

#### **Droplet digital PCR**

The frequency of large genomic deletions were quantified using EvaGreen-based ddPCR assay. The reaction mixture includes 20 ng of genomic DNA, 1x QX200 ddPCR EvaGreen supermix, and 100 nM primers for 20  $\mu\text{L}$  reaction. For absolute measure of deletions, we designed primers that amplify the sequences flanking the cut sites after targeted deletion. Control primers amplifying embryonic globin gene were used as loading control (EG). The percentage of deletion was calculated using the following formula:

$$\left(\frac{EAB}{EE}\right) * 100$$

where,

EAB is DNA copies/ $\mu\text{L}$  from primers flanking the cut sites of edited samples, and EE is DNA copies/ $\mu\text{L}$  from primers amplifying embryonic globin gene of edited samples.

The second approach involves the quantification of the individual cut sites of the deletion, normalized with the read outs from the unedited control samples.

$$\left(100 - \left(\frac{EA * \left(\frac{UE}{UA}\right)}{EE}\right) + \left(\frac{EB * \left(\frac{UE}{UB}\right)}{EE}\right)\right) * 100$$

Where,

EA – DNA copies/ $\mu\text{L}$  from primers flanking the cut site A of edited samples.

EB – DNA copies/ $\mu\text{L}$  from primers flanking the cut site B of edited samples.

EE - DNA copies/ $\mu\text{L}$  from primers amplifying embryonic globin gene of edited samples.

UA – DNA copies/ $\mu\text{L}$  from primers flanking the cut site A of unedited samples.

UB – DNA copies/ $\mu\text{L}$  from primers flanking the cut site B of unedited samples.

UE - DNA copies/ $\mu\text{L}$  from primers amplifying embryonic globin gene of unedited samples.

The indels at the individual cutsite were quantified using ICE analysis with the primers mentioned in Table S3. Primers used in ddPCR analysis are mentioned in Table S4.

#### **Hemoglobin and globin chain analysis using HPLC**

The gene-edited HUDEP-2 cell lines and CD34<sup>+ve</sup> HSPCs were collected on day 8 and day 20 of erythroid differentiation, respectively. The cells were sonicated for 60 s with 50% AMP in ice using ultrasonicator (Vibra-Cell) and centrifuged at 14,000 rpm for 5 min at 4°C. For hemoglobin HPLC, the protein lysate was analyzed for hemoglobin tetramer using G8 HPLC Analyzer (Tosoh). The globin chain analysis was performed using HPLC equipment with UV detector (Shimadzu) and the analysis was performed using LC Solutions<sup>TM</sup> software (Shimadzu) using the previously reported method.<sup>50</sup> Aeris Widepore 3.6  $\mu\text{m}$  XB-C18 25 cm 4.6 mm column behind a Security Guard UHPLC Widepore C18 4.6 mm guard column (Phenomenex<sup>TM</sup>) is used for chromatographic separation of the analytes. HPLC conditions include 0.1% trifluoroacetic acid (TFA), pH 3.0 (solvent A), mobile phase - 0.1% TFA in acetonitrile

(solvent B) with gradient elution at a flow rate of 1.0 mL/min and column temperature maintained at 70°C with runtime around 8 min and UV detection range of 190 nm was set for globin chain detection.

#### Western blot analysis

Approximately  $6 \times 10^6$  erythroblasts were collected on day 8 of erythroid differentiation. The lysates were prepared sonicating the cell pellets resuspended in RIPA buffer supplemented 1x protease and phosphatase inhibitor cocktail. Twenty micrograms of protein lysates resuspended in 1x Lamelli buffer were loaded to the wells of SDS-PAGE. The western blots were performed using the primary antibodies, anti-hemoglobin  $\alpha$  (1:1,000 dilution), anti-hemoglobin  $\beta$  (1:1,000 dilution), anti-hemoglobin  $\gamma$  (1:1,000 dilution), and anti-actin (1:1,000 dilution) along with anti-mouse immunoglobulin (Ig) G horseradish peroxidase (HRP) secondary antibodies. Densitometric analysis of the globin bands were performed by normalizing with  $\beta$ -actin. List of western blot antibodies used in the study were mentioned in [Table S7](#).

#### Transcriptome analysis

Total RNA was extracted using a Qiagen RNA isolation kit, quantified using Qubit RNA Assay HS, purity checked using QIAxpert, and RNA integrity was assessed on TapeStation using RNA HS ScreenTapes (Agilent, Cat# 5067-5579). NEB Ultra II Directional RNA-Seq Library Prep kit protocol was used to prepare libraries for total RNA sequencing (RNA-seq). Prepared libraries were quantified using Qubit High Sensitivity Assay (Invitrogen, Cat# Q32852). A cluster flow cell is loaded on Illumina HiSeq 4000 instrument to generate 60 M, 100 bp paired-end reads. Read Counts from mapped reads were obtained using Feature Counts. Differential expression analysis was performed using DESEQ2. GSEA was by GSEA software from the Broad Institute. A ranked list of differentially expressed genes from RNA-seq data was loaded into GSEA and tested against a list of genes documented from published reports. A heatmap for differentially regulated genes was generated using Morpheus (Broad Institute).

#### CAST-Seq analysis

CAST-Seq library preparation was performed as previously described.<sup>33</sup> Two technical replicates derived from two independent editing experiments were prepared and analyzed against a corresponding untreated control sample. We considered as relevant findings all sites identified in at least two out of four replicates with a read-to-CAST-Seq hit ratio of >10 to eliminate unspecific reads. CAST-Seq libraries were sequenced by NGS service provider Genewiz (part of Azenta Life Sciences). At Genewiz, sequencing was performed on an Illumina NovaSeq device collecting 2x 150 bp paired-end reads. The bioinformatics analysis was adapted to allow for concomitant input of more than one target site/guide RNA sequence. The oligo nucleotides used for CAST-Seq analysis are mentioned in [Table S8](#).

#### Micronucleus assay

Micronucleus assay was performed as previously described<sup>51</sup> following the published guidelines.<sup>52</sup> Briefly, the gene-edited HSPCs

were incubated with 10  $\mu$ M cytochalasin B for 23 h and fixed with methanol and stained with Giemsa stain. The images were captured using  $\times 40$  magnification using an Olympus upright microscope BX43.

#### KaryoStat assay

Gene-edited HSPCs were collected for genomic DNA isolation using PureLink Genomic DNA Mini Kit (catalog #K182000) and quantified using Qubit dsDNA assay. After digestion of 250 ng of genomic DNA using Nsp I restriction enzyme, the DNA was ligated with adapter and amplified. The DNA was fragmented followed by labeling with biotin and the labeled DNA was hybridized onto GeneChip arrays. GeneChip Fluidics Station 450 were used for washing and staining of Chips simultaneously scanned using GeneChip Scanner 3000 7 G. Data were analyzed using ChAS 3.2. The raw data were processed using Genotyping Console v4.0 and Chromosome Analysis Suite 3.2 with NetAffx na33.1 (UCSC GRCh37/hg19), and the output data were interpreted with the UCSC Genome Browser (<https://genome.ucsc.edu/>; GRCh37/hg19 assembly).

#### 4C analysis

4C was performed as per the protocol described in the literature with minor variations.<sup>53</sup> Cells (HUDEP-2 control and two PRR- $\beta$ E1 clones harboring biallelic deletion) were fixed with fresh formaldehyde (1.5%) and quenched with glycine (125 mM) followed by washes with ice-cold PBS (2 $\times$ ) and pelleted and stored at  $-80^\circ\text{C}$ . Lysis buffer (Tris-Cl pH 8.0 [10 mM], NaCl [10 mM], NP-40 [0.2%], PIC [1 $\times$ ]) was added to the pellets and were homogenized by Dounce homogenizer (15 stroked with pestle A followed by pestle B). The 3C digestion was performed with Csp6I (10 units, Thermofisher #ER0211) and ligation was performed by the T4 DNA ligase in 7.61 mL ligation mix (745  $\mu$ L 10% Triton X-100, 745  $\mu$ L 10x ligation buffer (500 mM Tris-HCl pH 7.5, 100 mM MgCl<sub>2</sub>, 100 mM DTT), 80  $\mu$ L 10 mg/mL BSA, 80  $\mu$ L 100 mM ATP, and 5.96 mL water). The ligated samples were de-crosslinked overnight then purified by PCI purification and subjected to ethanol precipitation and the pellet was eluted in TE (pH 8.0) to obtain the 3C library. The second 4C digestion was performed by DpnII (50 units, NEB) and the samples were ligated, purified, and precipitated similar to the 3C library to obtain the 4C library. The 4C library was subjected to RNaseA treatment and purified by the QIAquick PCR purification kit. The concentration of the library was then measured by Nanodrop and subjected to PCRs using the oligos for the respective viewpoints. The oligos used for the HBG2 viewpoint are mentioned in [Table S6](#). The samples were PCR purified and subjected to next-generation sequencing with Illumina HiSeq2500 using 50-bp single-end reads. Data analysis was performed using 4Cseqpipe (<https://github.com/changegene/4Cseqpipe>) using default parameters.

#### DATA AVAILABILITY

RNA datasets are available in the Gene Expression Omnibus repository (GEO: GSE201346). 4C datasets are available in the Gene Expression Omnibus repository (GEO: GSE201388). All data are available in the main text or the [supplemental information](#). Additional data



related to this paper may be requested from the corresponding author.

## SUPPLEMENTAL INFORMATION

Supplemental information can be found online at <https://doi.org/10.1016/j.omtn.2023.04.024>.

## ACKNOWLEDGMENTS

The authors thank the funders; Department of Biotechnology, government of India (BT/PR17316/MED/31/326/2015, BT/PR26901/MED/31/377/2017 and BT/PR31616/MED/31/408/2019 to ST), European Commission (HORIZON-RIA EDITSCD No. 101057659 to T.C.), ICMR-SRF fellowship (V.V., A.C.), CSIR-JRF fellowship (P.B.), and DST-INSPIRE fellowship (K.V.K.). The authors also thank Dr. Sowmya Pattabhi for help in designing the ddPCR strategy, Mr. Dhananjayan and Mr. Daniel Beno for ddPCR-related technical inputs, and the staffs of flow cytometry, animal facility, and core facilities for their support.

## AUTHOR CONTRIBUTIONS

Conceptualization: S.T., A.S., S.V., S.M., and K.M. Experiment execution and analysis: V.V., A.C., M.R., P.B., M.A., K.W., B.S., S.S., K.V.K., A.J., S.R., A.P., Y.N., R.P., G.A. Technical supervision: S.T., A.S., D.N., S.V., P.B., S.M., M.B. Manuscript – review & editing: V.V., S.T., A.S., T.C., S.V., S.M., and K.M. Funding acquisition: S.T. and T.C.

## DECLARATION OF INTERESTS

The authors declare no competing interests.

## REFERENCES

- De Sanctis, V., Kattamis, C., Canatan, D., Soliman, A.T., Eلسdfy, H., Karimi, M., Daar, S., Wali, Y., Yassin, M., Soliman, N., et al. (2017).  $\beta$ -thalassemia distribution in the old world: an ancient disease seen from a historical standpoint. *Mediterr. J. Hematol. Infect. Dis.* 9, e2017018.
- Colah, R., Italia, K., and Gorakshakar, A. (2017). Burden of thalassemia in India: the road map for control. *Pediatr. Hematol. Oncol. J.* 2, 79–84.
- Boonyawat, B., Monsereenusorn, C., and Traivaree, C. (2014). Molecular analysis of beta-globin gene mutations among Thai beta-thalassemia children: results from a single center study. *Appl. Clin. Genet.* 7, 253–258.
- Origa, R. (2017).  $\beta$ -Thalassemia. *Genet. Med.* 19, 609–619.
- Sundd, P., Gladwin, M.T., and Novelli, E.M. (2019). Pathophysiology of sickle cell disease. *Annu. Rev. Pathol.* 14, 263–292.
- Fitzhugh, C.D., Hsieh, M.M., Allen, D., Coles, W.A., Seamon, C., Ring, M., Zhao, X., Minniti, C.P., Rodgers, G.P., Schechter, A.N., et al. (2015). Hydroxyurea-increased fetal hemoglobin is associated with less organ damage and longer survival in adults with sickle cell anemia. *PLoS One* 10, e0141706.
- Musallam, K.M., Sankaran, V.G., Cappellini, M.D., Duca, L., Nathan, D.G., and Taher, A.T. (2012). Fetal hemoglobin levels and morbidity in untransfused patients with  $\beta$ -thalassemia intermedia. *Blood* 119, 364–367.
- Nunoon, M., Makarasara, W., Mushihiro, T., Setianingsih, I., Wahidiyat, P.A., Sripichai, O., Kumasaka, N., Takahashi, A., Svasti, S., Munkongdee, T., et al. (2010). A genome-wide association identified the common genetic variants influence disease severity in  $\beta$ 0-thalassemia/hemoglobin e. *Hum. Genet.* 127, 303–314.
- Masuda, T., Wang, X., Maeda, M., Canver, M.C., Sher, F., Funnell, A.P.W., Fisher, C., Suci, M., Martyn, G.E., Norton, L.J., et al. (2016). Gene regulation: transcription factors LRF and BCL11A independently repress expression of fetal hemoglobin. *Science* 351, 285–289.
- Canver, M.C., Smith, E.C., Sher, F., Pinello, L., Sanjana, N.E., Shalem, O., Chen, D.D., Schupp, P.G., Vinjamur, D.S., Garcia, S.P., et al. (2015). BCL11A enhancer dissection by Cas9-mediated in situ saturating mutagenesis. *Nature* 527, 192–197.
- Esrick, E.B., Lehmann, L.E., Biffi, A., Achebe, M., Brendel, C., Ciuculescu, M.F., Daley, H., MacKinnon, B., Morris, E., Federico, A., et al. (2021). Post-transcriptional genetic silencing of BCL11A to treat sickle cell disease. *N. Engl. J. Med.* 384, 205–215.
- Frangoul, H., Altshuler, D., Cappellini, M.D., Chen, Y.-S., Domm, J., Eustace, B.K., Foell, J., de la Fuente, J., Grupp, S., Handgretinger, R., et al. (2021). CRISPR-Cas9 gene editing for sickle cell disease and  $\beta$ -thalassemia. *N. Engl. J. Med.* 384, 252–260.
- Ringelhan, B., Acquaye, C.T., Oldham, J.H., Konotey-Ahulu, F.I., Yawson, G., Sukumaran, P.K., Schroeder, W.A., and Huisman, T.H. (1977). Homozygotes for the hereditary persistence of fetal hemoglobin: the ratio of G $\gamma$  to A $\gamma$  chains and biosynthetic studies. *Biochem. Genet.* 15, 1083–1096.
- Cianetti, L., Care, A., Sposi, N.M., Giampaolo, A., Calandrini, M., Petrini, M., Massa, A., Marinucci, M., Mavilio, F., Ceccanti, M., et al. (1984). Association of heterocellular HPFH-i-thalassemia, and a 0-thalassaemia: haematological and molecular aspects. *J. Med. Genet.* 21, 263–267.
- Steinberg, M.H. (2020). Fetal hemoglobin in sickle hemoglobinopathies: high HbF genotypes and phenotypes. *J. Clin. Med.* 9, 3782.
- Venkatesan, V., Srinivasan, S., Babu, P., and Thangavel, S. (2020). Manipulation of developmental Gamma-globin gene expression: an approach for healing hemoglobinopathies. *Mol. Cell Biol.* 41, e00253-20.
- Ye, L., Wang, J., Tan, Y., Beyer, A.L., Xie, F., Muench, M.O., and Kan, Y.W. (2016). Genome editing using CRISPR-Cas9 to create the HPFH genotype in HSPCs: an approach for treating sickle cell disease and  $\beta$ -thalassemia. *Proc. Natl. Acad. Sci. USA* 113, 10661–10665.
- Antoniani, C., Meneghini, V., Lattanzi, A., Felix, T., Romano, O., Magrin, E., Weber, L., Pavani, G., El Hoss, S., Kurita, R., et al. (2018). Induction of fetal hemoglobin synthesis by CRISPR/Cas9-mediated editing of the human b-globin locus. *Blood* 131, 1960–1973.
- Topfer, S.K., Feng, R., Huang, P., Ly, L.C., Martyn, G.E., Blobel, G.A., Weiss, M.J., Quinlan, K.G.R., and Crossley, M. (2022). Disrupting the adult globin promoter alleviates promoter competition and reactivates fetal globin gene expression. *Blood* 139, 2107–2118.
- Joly, P., Lacan, P., Garcia, C., Couprie, N., and Francina, A. (2009). Identification and molecular characterization of four new large deletions in the  $\beta$ -globin gene cluster. *Blood Cells Mol. Dis.* 43, 53–57.
- Changri, K., Akkarapathumwong, V., Jamsai, D., Winichagoon, P., and Fucharoen, S. (2006). Molecular mechanism of high hemoglobin F production in Southeast Asian-type hereditary persistence of fetal hemoglobin. *Int. J. Hematol.* 83, 229–237.
- Camaschella, C., Serra, A., Gottardi, E., Alfaro, A., Revello, D., Mazza, U., and Saglio, G. (1990). A new hereditary persistence of fetal hemoglobin deletion has the breakpoint within the 3' beta-globin gene enhancer. *Blood* 75, 1000–1005.
- Kulozik, A.E., Yarwood, N., and Jones, R.W. (1988). The Corfu  $\alpha\beta^0$  thalassemia: a small deletion acts at a distance to selectively abolish  $\beta$  globin gene expression. *Blood* 71, 457–462.
- Anand, R., Boehm, C.D., Kazazian, H.H., Jr., and Vanin, E.F. (1988). Molecular characterization of a  $\beta$ 0 -thalassemia resulting from a 1.4 kilobase deletion. *Blood* 72, 636–641.
- Dimovski, A.J., Efremov, D.G., Jankovic, L., Plaseska, D., Juricic, D., and Efremov, G.D. (1993). A  $\beta^0$  -thalassaemia due to a 1605 bp deletion of the 5'  $\beta$ -globin gene region. *Br. J. Haematol.* 85, 143–147.
- Métais, J.Y., Doerfler, P.A., Mayuranathan, T., Bauer, D.E., Fowler, S.C., Hsieh, M.M., Katta, V., Keriwala, S., Lazzarotto, C.R., Luk, K., et al. (2019). Genome editing of HBG1 and HBG2 to induce fetal hemoglobin. *Blood Adv.* 3, 3379–3392.
- McIntosh, B.E., Brown, M.E., Duffin, B.M., Maufort, J.P., Vereide, D.T., Slukvin, I.I., and Thomson, J.A. (2015). Nonirradiated NOD.B6.SCID Il2ry<sup>-/-</sup> Kit(W41/W41) (NBSGW) mice support multilineage engraftment of human hematopoietic cells. *Stem Cell Rep.* 4, 171–180.
- El Hoss, S., Cochet, S., Godard, A., Yan, H., Dussiot, M., Frati, G., Boutonnat-Faucher, B., Laurance, S., Renaud, O., Joseph, L., et al. (2020). Fetal hemoglobin rescues ineffective erythropoiesis in sickle cell disease. *Haematologica* 136, 14–15.

29. Yang, Z., Cui, Q., Zhou, W., Qiu, L., and Han, B. (2019). Comparison of gene mutation spectrum of thalassemia in different regions of China and Southeast Asia. *Mol. Genet. Genomic Med.* 7, 680.
30. Sinha, S., Black, M.L., Agarwal, S., Colah, R., Das, R., Ryan, K., Bellgard, M., and Bittles, A.H. (2009). Profiling  $\beta$ -thalassaemia mutations in India at state and regional levels: implications for genetic education, screening and counselling programmes. *Hugo J.* 3, 51–62.
31. Arlet, J.-B., Ribeil, J.-A., Guillem, F., Negre, O., Hazoume, A., Marcion, G., Beuzard, Y., Dussiot, M., Moura, I.C., Demarest, S., et al. (2014). HSP70 sequestration by free  $\alpha$ -globin promotes ineffective erythropoiesis in  $\beta$ -thalassaemia. *Nature* 514, 242–246.
32. Leibowitz, M.L., Papatthanasios, S., Doerfler, P.A., Blaine, L.J., Sun, L., Yao, Y., Zhang, C.Z., Weiss, M.J., and Pellman, D. (2021). Chromothripsis as an on-target consequence of CRISPR–Cas9 genome editing. *Nat. Genet.* 53, 895–905.
33. Turchiano, G., Andrieux, G., Klermund, J., Blattner, G., Pennucci, V., el Gaz, M., Monaco, G., Poddar, S., Mussolino, C., Cornu, T.I., et al. (2021). Quantitative evaluation of chromosomal rearrangements in gene-edited human stem cells by CAST-Seq. *Cell Stem Cell* 28, 1136–1147.e5.
34. Kleinstiver, B.P., Pattanayak, V., Prew, M.S., Tsai, S.Q., Nguyen, N.T., Zheng, Z., and Joung, J.K. (2016). High-fidelity CRISPR–Cas9 nucleases with no detectable genome-wide off-target effects. *Nature* 529, 490–495.
35. Vinjamur, D.S., Bauer, D.E., and Orkin, S.H. (2018). Recent progress in understanding and manipulating haemoglobin switching for the haemoglobinopathies. *Br. J. Haematol.* 180, 630–643.
36. Ma, S.P., Xi, H.R., Gao, X.X., Yang, J.M., Kurita, R., Nakamura, Y., Song, X.M., Chen, H.Y., and Lu, D.R. (2021). Long noncoding RNA HBBP1 enhances  $\gamma$ -globin expression through the ETS transcription factor ELK1. *Biochem. Biophys. Res. Commun.* 552, 157–163.
37. Ivaldi, M.S., Diaz, L.F., Chakalova, L., Lee, J., Krivega, I., and Dean, A. (2018). Fetal  $\gamma$ -globin genes are regulated by the BGLT3 long noncoding RNA locus. *Blood* 132, 1963–1973.
38. Lamsfus-Calle, A., Daniel-Moreno, A., Antony, J.S., Epting, T., Heumos, L., Baskaran, P., Admard, J., Casadei, N., Latifi, N., Siegmund, D.M., et al. (2020). Comparative targeting analysis of KLF1, BCL11A, and HBG1/2 in CD34+ HSPCs by CRISPR/Cas9 for the induction of fetal hemoglobin. *Sci. Rep.* 10, 10133.
39. Chung, J.E., Magis, W., Vu, J., Heo, S.-J., Wartiovaara, K., Walters, M.C., Kurita, R., Nakamura, Y., Boffelli, D., Martin, D.I.K., et al. (2019). CRISPR–Cas9 interrogation of a putative fetal globin repressor in human erythroid cells. *PLoS One* 14, e0208237.
40. Shen, Y., Verboon, J.M., Zhang, Y., Liu, N., Kim, Y.J., Marglous, S., Nandakumar, S.K., Voit, R.A., Fiorini, C., Ejaz, A., et al. (2021). A unified model of human hemoglobin switching through single-cell genome editing. *Nat. Commun.* 12, 4991.
41. Boontanrart, M.Y., Schröder, M.S., Stehli, G.M., Banović, M., Wyman, S.K., Lew, R.J., Bordi, M., Gowen, B.G., DeWitt, M.A., and Corn, J.E. (2020). ATF4 regulates MYB to increase  $\gamma$ -globin in response to loss of  $\beta$ -globin. *Cell Rep.* 32, 107993.
42. Ramadier, S., Chalumeau, A., Felix, T., Othman, N., Aknoun, S., Casini, A., Maule, G., Masson, C., De Cian, A., Frati, G., et al. (2022). Combination of lentiviral and genome editing technologies for the treatment of sickle cell disease. *Mol. Ther.* 30, 145–163.
43. Humbert, O., Radtke, S., Samuelson, C., Carrillo, R.R., Perez, A.M., Reddy, S.S., Lux, C., Patabhi, S., Scheffer, L.E., Negre, O., et al. (2019). Therapeutically relevant engraftment of a CRISPR–Cas9-edited HSC-enriched population with HbF reactivation in nonhuman primates. *Sci. Transl. Med.* 11, eaaw3768.
44. Karuppusamy, K.V., Demosthenes, J.P., Venkatesan, V., Christopher, A.C., Babu, P., Azhagiri, M.K., Jacob, A., Ramalingam, V.V., and Rangaraj, S. (2022). The CCR5 gene edited CD34 + CD90 + hematopoietic stem cell population serves as an optimal graft source for HIV gene therapy. *Front. Immunol.* 13, 1–15.
45. Christopher, A.C., Venkatesan, V., Karuppusamy, K.V., Srinivasan, S., Babu, P., Azhagiri, M.K., C, K., Bagchi, A., Rajendiran, V., Ravi, N.S., et al. (2021). Preferential expansion of human CD34+CD133+CD90+ hematopoietic stem cells enhances gene-modified cell frequency for gene therapy. *Hum. Gene Ther.* 1–33.
46. Venkatesan, V., Christopher, A.C., Karuppusamy, K.V., Babu, P., Kumar, M., Alagiri, K., and Thangavel, S. (2022). CRISPR/Cas9 gene editing of hematopoietic stem and progenitor cells for gene therapy applications. *J. Vis. Exp.* 1–20. <https://doi.org/10.3791/64064>.
47. Trakarnsanga, K., Griffiths, R.E., Wilson, M.C., Blair, A., Satchwell, T.J., Meinders, M., Cogan, N., Kupzig, S., Kurita, R., Nakamura, Y., et al. (2017). An immortalized adult human erythroid line facilitates sustainable and scalable generation of functional red cells. *Nat. Commun.* 8, 14750–14757.
48. Chang, K.H., Smith, S.E., Sullivan, T., Chen, K., Zhou, Q., West, J.A., Liu, M., Liu, Y., Vieira, B.F., Sun, C., et al. (2017). Long-term engraftment and fetal globin induction upon BCL11A gene editing in bone-marrow-derived CD34+ hematopoietic stem and progenitor cells. *Mol. Ther. Methods Clin. Dev.* 4, 137–148.
49. Zeng, J., Wu, Y., Ren, C., Bonanno, J., Shen, A.H., Shea, D., Gehrke, J.M., Clement, K., Luk, K., Yao, Q., et al. (2020). Therapeutic base editing of human hematopoietic stem cells. *Nat. Med.* 26, 535–541.
50. Loucari, C.C., Patsali, P., Van Dijk, T.B., Stephanou, C., Papisavva, P., Zanti, M., Kurita, R., Nakamura, Y., Christou, S., Sitarou, M., et al. (2018). Rapid and sensitive assessment of globin chains for gene and cell therapy of hemoglobinopathies. *Hum. Gene Ther. Methods* 29, 60–74.
51. Mosesso, P., and Cinelli, S. (2019). In vitro cytogenetic assays: chromosomal aberrations and micronucleus tests. *Methods Mol. Biol.* 2031, 79–104.
52. Fenech, M., Chang, W.P., Kirsch-Volders, M., Holland, N., Bonassi, S., and Zeiger, E.; HUMAN MICRONUCLEUS PROJECT (2003). HUMN project: detailed description of the scoring criteria for the cytokinesis-block micronucleus assay using isolated human lymphocyte cultures. *Mutat. Res.* 534, 65–75.
53. Van De Werken, H.J.G., Landan, G., Holwerda, S.J.B., Hoichman, M., Klous, P., Chachik, R., Splinter, E., Valdes-Quezada, C., Öz, Y., Bouwman, B.A.M., et al. (2012). Robust 4C-seq data analysis to screen for regulatory DNA interactions. *Nat. Methods* 9, 969–972.